Universidade de Aveiro
2016

Departamento de Engenharia Mecânica

Paulo Miguel Trindade Santos

Estratégias para o melhoramento das propriedades mecânicas de compósitos baseados em cortiça aglomerada

Universidade de Aveiro
2016

Departamento de Engenharia Mecânica

Paulo Miguel Trindade Santos

Estratégias para o melhoramento das propriedades mecânicas de compósitos baseados em cortiça aglomerada

Dissertação apresentada à Universidade de Aveiro para cumprimento dos requisitos necessários à obtenção do grau de Mestre em Engenharia Mecânica, realizada sob a orientação científica de Ricardo José Alves de Sousa, Professor Auxiliar no Departamento de Engenharia Mecânica da Universidade de Aveiro e Paula Alexandrina de Aguiar Pereira Marques, equiparada a Investigador Principal no Departamento de Engenharia Mecânica da Universidade de Aveiro.

Dedico esta dissertação à minha família e amigos.

O júri / The jury

Presidente / President

Professor Doutor Robertt Angelo Fontes Valente
Professor Associado no Departamento de Engenharia Mecânica da Universidade do Aveiro

Vogais / Committee

Professor Doutor Ricardo José Alves de Sousa
Professor Auxiliar no Departamento de Engenharia Mecânica da Universidade de Aveiro

Professor Doutor José Luís Soares Esteves
Professor Auxiliar no Departamento de Engenharia Mecânica da Faculdade de Engenharia da Universidade do Porto

Agradecimentos / Acknowledgements

Um agradecimento muito especial aos meus orientadores Professor Doutor Ricardo Sousa e Doutora Paula Marques, pela sua orientação, apoio, disponibilidade, conhecimento transmitido, opiniões, críticas e todas as palavras de incentivo. Um muito obrigado por toda a dedicação e trabalho.

Um especial obrigado à Susana Pinto e Daniel Afonso pela sua ajuda e apoio nos seus respetivos campos científicos.

Ao Professor Doutor António Pereira e aos colegas e amigos Sílvia Carvalho e Arménio Lima por toda a ajuda e apoio prestados na campanha experimental desta dissertação.

À Professora Doutora Mónica Oliveira, pelo espaço e equipamentos cedidos.

A todos os colegas do GRIDS, especialmente ao meu colega Fábio Fernandes pela disponibilidade e conselhos.

Ainda e não menos importante, um grande agradecimento à minha família e amigos pelo amor, coragem e apoio.

Palavras-chave

Materiais celulares naturais; cortiça aglomerada; testes mecânicos; impacto; compressão uniaxial; absorção de energia; materiais sustentáveis; materiais à base de carbono; grafeno; oxido de grafeno; nanocompósitos.

Resumo

Devido a uma maior preocupação ambiental, produtos à base de cortiça têm ganho relevo nas mais diversas áreas.

As sobras da produção de rolhas e outros produtos de cortiça são geralmente triturados e aglomerados. O produto resultante é denominado cortiça aglomerada, sendo este um material com grande variedade de aplicações. A cortiça aglomerada é um bom isolante térmico e acústico, tendo ainda boa capacidade de absorver vibrações e energia de impactos.

Todavia, a literatura científica tem apresentado a cortiça aglomerada de modo muito genérico e pouco especifico, definindo a densidade e o tamanho do grão utilizado na produção do aglomerado, como os dois principais parâmetros que influenciam as propriedades da cortiça aglomerada.

Muitos estudos efetuados, que recorreram a cortiça aglomerada, são vagos nas informações que fornecem sobre o aglomerado de cortiça utilizado, ou mesmo em alguns casos estas informações encontram-se omissas.

É o objetivo desta dissertação, demonstrar que existem outros parâmetros que influenciam as propriedades mecânicas da cortiça aglomerada e quantificar a sua influência. Para o efeito, uma campanha experimental com base em testes de compressão quase-estáticos e testes dinâmicos foi planeada e executada.

Ainda como objetivo desta dissertação, foi estudar a influência da incorporação de nano materiais, nomeadamente grafeno e óxido de grafeno, como reforço na cortiça aglomerada. Com esse objetivo, uma segunda campanha experimental foi planeada e executada.

Com o estudo dos dados obtidos foi possível provar que alterando os parâmetros de produção da cortiça aglomerada, é possível adequar as suas propriedades à aplicação a que destina.

Keywords

Natural cellular materials; agglomerated cork; mechanical tests; impact; uniaxial compression, energy absorption; sustainable materials. carbon-based materials; graphene; graphene oxide; nanocomposites.

Abstract

The use of cork material has been quickly spreading over the last years due to more care taken to environmental issues. The scrap coming from the production of traditional wine stopper or from the production of other cork products is generally triturated and agglomerated. The so-called agglomerated cork material has been finding a wide range of applications, being a good thermal and acoustic insulator, vibration and impact absorber.

Nevertheless, scientific literature has been addressing agglomerated cork in a very general way and defining density and grain size as the two main defining parameters. Many studies that used agglomerated cork, failed to specify the parameters that were used in its production.

This dissertation aims to show that, apart from density and grain size, there are other parameters, such as binder type or its quantity, may also have a very significant effect on the mechanical properties of cork in agglomerated form. To this end, the whole production process is detailed and a campaign of static and dynamic tests is carried out. Another goal of this dissertation was to determine the influence of the incorporation of nanomaterials, namely graphene and graphene oxide, as reinforcement on the agglomerated cork. With that goal, a second experimental campaign was planned and carried out. Consisting of quasi-static compression tests and burn tests.

With the results obtain it was possible to conclude, that by altering the production parameters of the agglomerated cork it is possible to change its properties, to meet the requirements of the intended application.

Contents

List of Figures

List of Tables

Chapter 1
State of the Art

1.1 Introduction

Cellular materials have been used in many applications, from aerospace to construction, any application where impact energy absorption, thermal insulation or sound insulation is needed [1],[2]. Cellular materials can be divided into several categories, natural, synthetic, open cell and closed cell [3]. Both synthetic and natural have similar properties that are intrinsic to all cellular materials.

Synthetic cellular materials are used in a great variety of products, for example, in helmet liners to absorb impact energy in case of an accident, preventing injuries to the user [4][5]. For this particular kind of application, several mechanical properties must be taken into account. Although energy absorption is undoubtedly one of those properties, it is by far not the only one. Other considerations must be taken, such as weight, volume, multi-impact behaviour, generated acceleration and more. Besides all the similarities, due to its different constitutions and origins, they deliver different responses when subjected to impact [6]. Synthetic cellular materials are capable of absorbing more energy and produce considerable lower acceleration peaks for single impact applications. In the case of a second impact in the same area, the protection level offered by synthetic materials like expanded polystyrene (EPS) or expanded polypropylene (EPP) is minimal since the material deforms permanently without elastic recovery [6].

Cork is capable of absorbing considerable amounts of energy. It has mainly viscoelastic behaviour, so the mechanical response to subsequent impacts is kept virtually unchanged. The material's response to different types of load has been attracting the attention of many researchers looking for potential new applications for this material. Several studies have focused on the fundamental aspects of cork's mechanical behaviour under quasi-static axial compressive loading [7],[8],[9],[10].

The material's mechanical behaviour depends on several factors, starting from its origin, production method, density, and structure. Regarding natural cork, some studies were performed to ascertain the influence of some of these variables in its final mechanical properties [11].

However, in which concerns agglomerated cork, the possibility to change some production parameters to tailor mechanical response under quasi-static and dynamic load remains an open question. Doing so, it is the main objective of this study to determine the influence of production parameters such as binder type, its quantity, cork grain size, agglomerate density and use of reinforcement materials on the mechanical properties of the agglomerated cork. For this purpose, three different binders, three distinct binder amounts, three different agglomerated densities, two

different grain sizes and two different reinforcement nano-fillers were tested, in order conclude about their influence on the final agglomerated cork mechanical properties and give insights about the best way to tailor up these properties.

1.2 Cellular Materials – Mechanical properties

Cellular materials exhibit properties that make them suitable for applications where impact absorption is needed. When cellular materials are subjected to uniaxial compression, it is possible to identify three distinct stages on the stress-strain curve as exemplified in Figure 1.1.

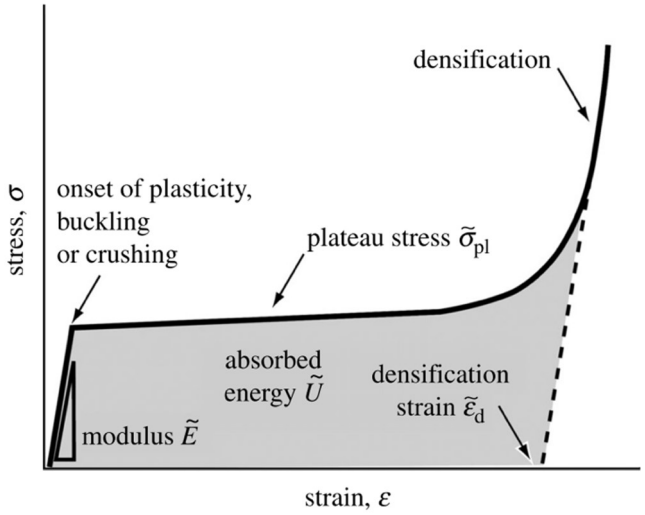

Figure 1.1: A stress–strain curve of a cellular solid [12].

For small deformations, the material has a linear elastic behaviour. For a homogeneous solid material subjected to a load in the linear elastic range, it is easy to determine its deformation with a certain degree of precision based on its mechanical properties, namely the Young modulus.

In the case of cellular materials, the mechanical properties can be influenced by several factors, such as the geometry of its cells, the properties of the cell walls material and by its relative density.

For greater deformations that exceed the linear elastic limit of the cellular material but without reaching the densification stage, the material behaves in a way that can be better described as viscoelastic. In this stage, the cell walls are subjected to stress, and as a result, they bend, much like a beam subjected to a load. In the viscoelastic range, the material can suffer further deformation at an almost constant value of stress, this behaviour can be observed in the stress-strain curve (Figure 1.1), as a horizontal line that resembles a plateau.

Depending on the cellular material, three distinct situations can occur. When the material that constitutes the cellular walls reach its elastic limit, it can demonstrate different behaviours, the cell edges yield plastically, buckle or fracture (Figure 1.2 and Figure 1.3).

When the plastic limit of the cell wall's material is immediately after its elastic limit, the cell wall's material reaches its rupture point. In this situation, the cellular material will still deform at a constant stress value, a plateau will still be observed resulting from the gradual rupture of the cellular walls.

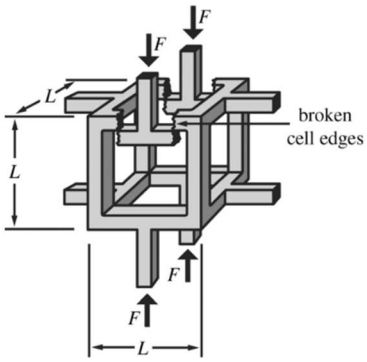

Figure 1.2: A brittle foam collapses by the successive fracturing of the cell edges. Ceramic foams generally present this collapse mechanism [12].

The downside of deforming the cell wall's material pass its rupture point is that it will not recover its initial properties, and this makes these materials not suitable for applications when multiple impact absorption is required.

Contrary to the situation aforesaid, when the plastic limit of the cell wall's material is not immediately after its linear elastic limit, the material also deforms at an almost constant value of stress, exhibiting a plateau on the stress-strain curve. The difference is that when the load on the cellular material is withdrawn, the material regains its initial properties and geometry. Making it ideal for situations where multiple impacts are expected.

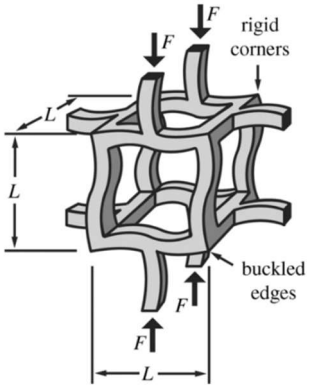

Figure 1.3: An elastomeric foam collapses by the elastic buckling of the cell edges [12].

At last, for greater deformations, the cellular material reaches the densification stage. At this point, the cellular material is so tightly compressed that the cell walls touch each other. This stage can be characterized by an abrupt rise of the stress values for small deformations.

For this reason, when conceiving project design, it is very important to carefully choose the cellular material that is more suited for a given mechanical requirement. Although there is still room to absorb

more impact energy in the densification stage, the downside of doing so is a steep increase in the values of accelerations. When doing a project where biomechanical behaviours must be taken into account, letting the values of acceleration spike is not an option, since the objective is to protect the human body.

1.3 Cork

"Quercus Suber L. is the botanical name for a slow growing, evergreen oak that flourishes only in specific regions of the Western Mediterranean (Portugal, Spain, Southern France, part of Italy, North Africa) and China. This tree requires a great deal of sunlight and a highly unusual combination of low rainfall and somewhat high humidity. Europe has about 60% of the total production area (cork forests) and produces more than 80% of the world's cork. Portugal is the major cork producer and processes about three-quarters of all the cork." [13].

Cork is a natural cellular material that constitutes the outer shell of the cork tree. The tree's trunk and branches are covered with a protective shell, which due to its properties is harvested periodically, usually 9-10 years, after they reach 25 cm in diameter, generally in the spring or summer. After the harvest, the tree will be left untouched for 9 years, in order to re-grow its bark [14].

Cork is produced by a cellular tissue named phellogen. When the cork is extracted this tissue is damaged and consequently dies. Then it is replaced by a new layer of phellogen, named traumatic phellogen, within 25 to 35 days, and after 50 days the first new cells of cork are produced. [15]

The phellogen is much more active when the tree is young. Consequently young trees produce more cork than older trees. The level of activity of the phellogen also varies according to different seasons. The period of greater activity is during April to October and is known as the phellogenium period. During the winter moths, there is a standstill in the production, this can be observed in visible dark zones (Figure 1.4)

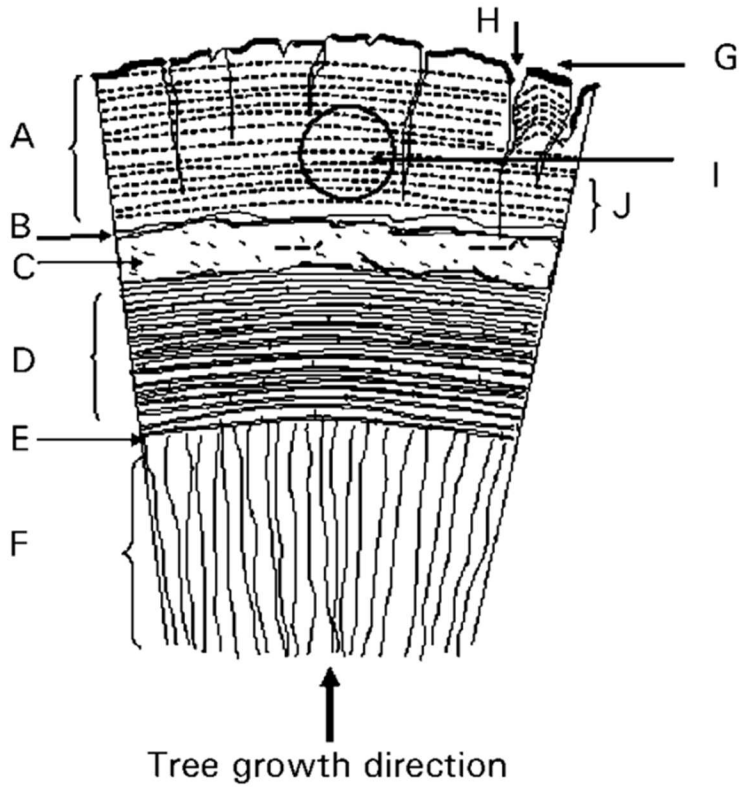

Figure 1.4: Schematic representation of axial section of cork oak tree; (A) cork (suberose tissue), (B) subero-phellogenic change, (C) phellogenium, (D) liber tissue, (E) liberwood change, (F) wood, (G) bark, (H) lenticular channels, (I) area for stopper production, (J) annual growth rings [13].

The main function of cork or phellem, the botanical designation of this vegetable tissue, is to act as a barrier between the atmosphere and the cortex of the stem, and the lenticels (Figure 1.4. H) provides a mean of mass transfer, for water and gasses.

1.3.1 Cork Structure

Cork, as a natural material, is not always uniform. Some properties vary depending on several factors. For instance, the density of the cork can vary with its age, type (virgin or reproduction) and treatment (natural or boiled). Generally, the density can vary between 120-240 kg/m^3. Also, the lenticular channel can influence the density of the cork. The cell walls are constituted by suberin (approximately 40%), lignin (22%), polysaccharides (18%) and extractables (15%). Virgin cork

contains more suberin, waxes, and fats, than the secondary cork and amadia cork generated after the extraction of the virgin cork.

The season of the year on which the cork bark grows influences the structure of the cork. For instance, cells formed during spring are taller, with thinner walls. Consequently, spring cells are less dense than an autumn cell. The porosity and growing rate also influence the density and geometry of the cell, especially its height. Although cork cells have a rectangular appearance, generally they have on average six sides.

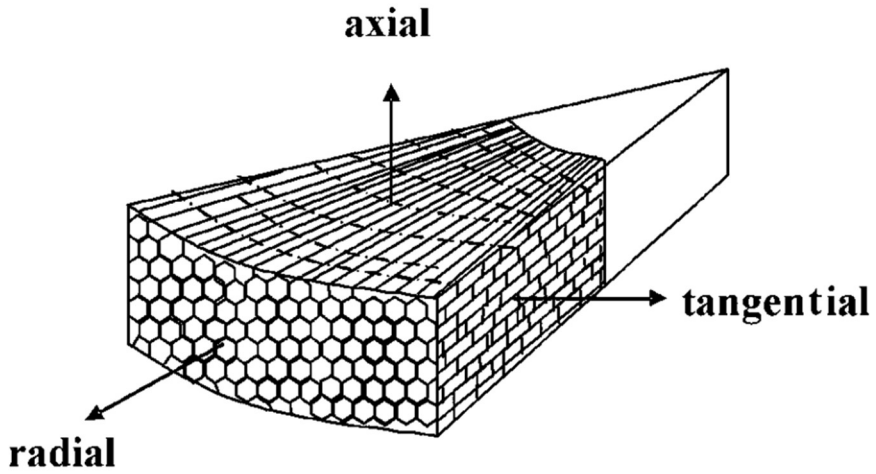

Figure 1.5: Cellular structure of natural cork [13].

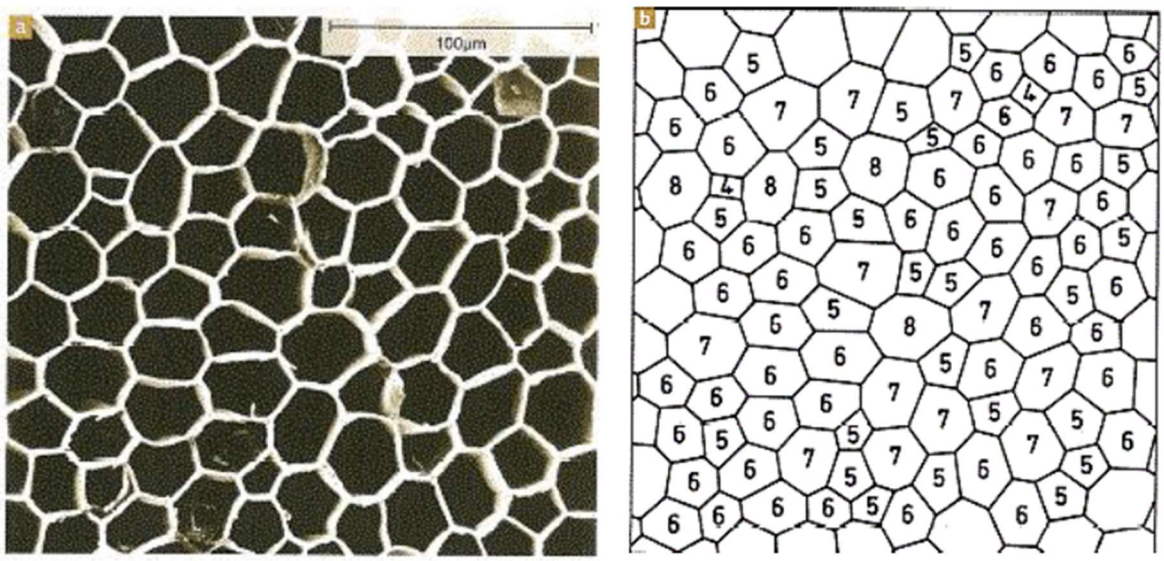

Figure 1.6: Tangential Section of amadia cork taken with scanning electron microscope [16].

Cork as an alveolar structure, that resembles a honeycomb, with close and hollow cells that contain on its interior gas, presumably air. The material that constitutes the cell walls is fairly homogeneous.

Although, due to its structural arrangement, natural cork is an anisotropic material, since the disposition of the cells varies according to the direction (Figure 1.5).

1.3.2 Production of cork

The *Quercus Suber L* is a tree with a slow grows and great longevity, being able to live 250 to 350 years, sometimes even more. Although due to the aforesaid reduction of cork production, the extraction of cork is limited to 150 to 200 years old trees. There is also a limit on how young a tree can be these restrictions are based not on the age of the tree in itself, but rather in its physical dimensions (25cm in diameter). What in the case of this species of tree correlates to an age of 20 to 35 years.

When the tree reaches the minimum size requirements, the cork is harvest for the first time. This cork is named virgin cork (Figure 1.7.a), and it is the protective shell of the cork tree since it was planted. This cork cannot be use for many applications since it has furrows and clefts, due to the accentuated radial grow of the tree in its first years. Generally, this cork is mashed and used to produce granular cork for cork agglomerates. The second cork extracted is named secondary cork, and this cork presents much of the defects that the virgin cork has. This one is also not suitable for the majority of applications, being instead used for the production of agglomerated cork. Finally, after the removal of this layer of cork, the next layer of cork produced by the tree is much more uniform, absent of furrows and clefts, or very small ones. This last type of cork is named *amadia* cork (Figure 1.7.b) and is this type of cork that is used in applications where it is important to have a homogeneous cork, such as in beverage's stoppers.

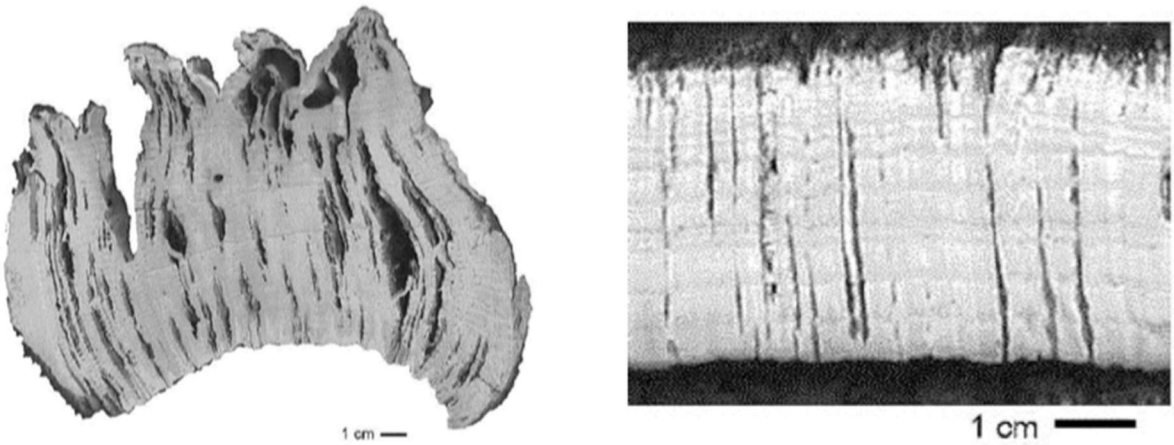

(a) (b)

Figure 1.7: Virgin cork (a) and *amadia* cork (b) [17].

After the extraction of cork, the first step is to treat the cork planks with water vapor. This allows the softening of the cork planks and makes possible the straightening of the otherwise bent planks. Then the cork planks must be boiled, to make it more malleable and fully expand the lenticels [13]. Before the boiling process the cork cells are collapsed, but due to the gas on the interior of the cork cell, when this is boiled, the gas heats and expand, stretching the cork cells, producing a much more uniform structure [18].

In the cork industry there is a lot of waste, the virgin cork, secondary cork and small pieces of *amadia* cork, that cannot be used in the direct manufacturing of products, so they are mashed into small grains that then are separated by density and size. Afterward, these grains are mixed with a polyurethane (PU) agglomerating and a catalyst agent and then shaped into the desired form that best suits the application for which is intended, from this process results agglomerated cork (AC).

There is also another way to process the grains of cork, they can be expanded at high temperatures with the addition of water, not being necessary the use of a polymeric agglomerating agent. The aggregation of the grains of cork is guaranteed by the natural suberin present in the cork. This type of cork is known as expanded cork (EC) or black cork (Figure 1.8).

Figure 1.8: Expanded cork.

Cork is one of the oldest resources of humanity, and its properties have proved useful in several applications. With the technological evolution, the number of application as grown as the cork possesses a set of special properties.

1.3.3 Natural *vs* synthetic

Cellular materials have been used in many applications, from aerospace to construction, basically, for any application where impact energy absorption, thermal insulation or sound insulation is needed. Cellular materials can be divided into several categories, natural cellular materials, synthetic cellular materials, open cell and closed cell cellular materials. The former division will not be addressed in this document.

Both synthetic and natural have similar intrinsic properties common to all cellular materials, regarding their mechanical properties when subjected to compression. As already mentioned, cellular materials exhibit three stages, where the second stage correspond to a characteristic plateau, where in the case of impact, most of the energy is absorbed. Besides all these similarities, due to its different constitutions and origins, they can express different behaviors when subjected to impact.

Synthetic cellular materials are used in a great variety of products, for example, in helmet liners in order to absorb impact energy in case of an accident, preventing injuries to the user. For this kind of application, several mechanical properties must be taken into account. Although energy absorption is one of those properties, it is not the only one. Other considerations must be taken, such as weight, density, ratio, multi-impact behavior, generated acceleration and more.

To further explore the differences between natural and synthetic cellular materials, some researchers tested different cellular materials, in different impact absorption conditions [6]. From the materials chosen, two were natural cellular materials, namely agglomerated cork (AC) and expanded cork (EC) and the other two were synthetic cellular materials, expanded polystyrene (EPS) and expanded polypropylene (EPP). To do a comprehensive analysis of the materials in analysis, the researchers subjected the materials to different types of loading. The first test was a quasi-static load performed at a very low speed. It was concluded that for this type of loading, synthetic cellular materials present a kind of behaviour that is more favorable and resembles more the behaviour of a perfect cellular material, with a steep increase in stress in the linear elastic range and a much more pronounced plateau, reaching densification later than natural cellular materials.

Looking at the results of the quasi-static tests, one can wrongly conclude that synthetic cellular materials are superior to natural cellular materials. It is only when the samples are dynamically tested that a broader picture of the behaviour of natural and synthetic materials starts to emerge.

On the dynamic tests performed by Fernandes et al, the samples of the different cellular materials were subjected to a multi-impact scenario, with a guided impactor of 5kg and 10kg. These tests were set to analyze the behaviour of cellular materials subjected to impact in a more realistic way, with a special attention on the variation of the samples properties on consecutive impacts and on the acceleration generated by the impact [6].

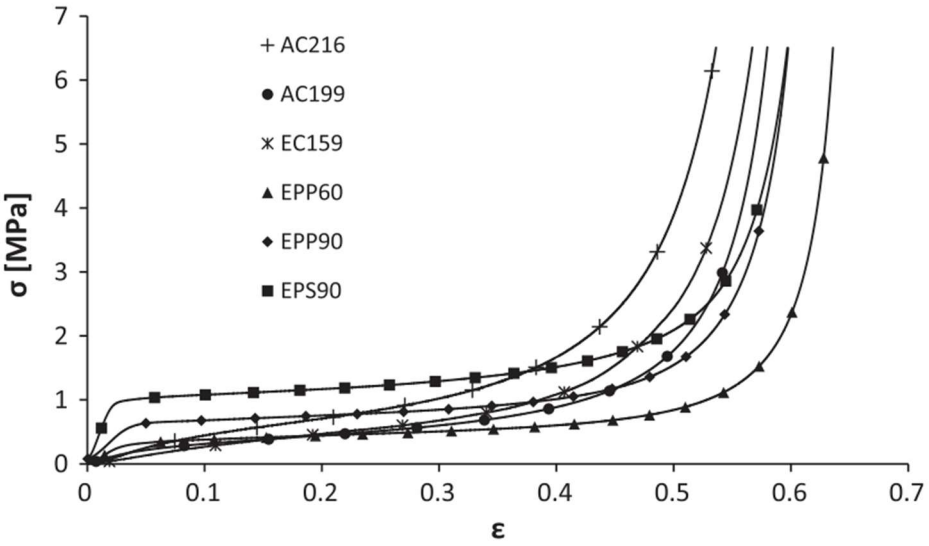

Figure 1.9: Synthetic foams and agglomerated cork stress–strain curves [6].

It was possible to observe that natural cellular materials, in this case, cork are indeed more suitable for multiple impact scenarios (see Figure 1.10). The degradation of the cork samples, both agglomerated cork and expanded cork, was almost negligible. By contrast, some samples of synthetic cellular materials, namely EPP, were destroyed on the first impact, making it impossible to perform a second test. Although the majority of synthetic samples were able to withstand a second impact, the degradations of their properties due to the first impact, were patently obvious. For the second impact, the values of acceleration spiked, contrarily the cork samples were able to maintain most of its initial properties, even after 4 or 5 impacts [6].

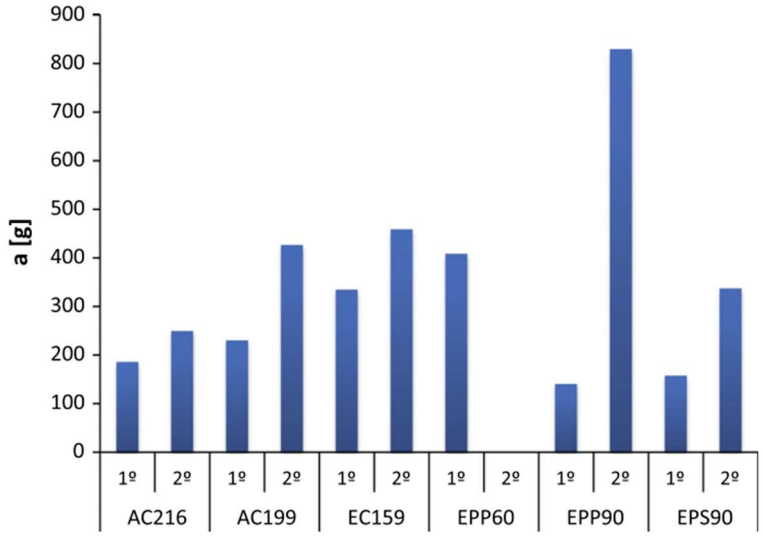

Figure 1.10: Mean acceleration peak value for both impacts (EPP60 missing since it was destroyed after the first impact) [6].

1.3.4 Factors that influence natural cork properties

Some research was made in regard to the properties of natural cork, when subjected to mechanical solicitations. To better understand the mechanical properties of cork, Anjos et al. studied the influence of several factors on natural cork's properties when subjected to quasi-static compression[11]. The variables studied were the quality, density, and porosity of the cork, as well as the direction of the compression, relative to the cork's structure.

To study the influence of the cork quality, two commercial planks of different qualities were tested in uniaxial compression at three distinct directions. The results were presented by stress-strain curves. The results showed that the quality of the cork had no influence in the values of stress until 50% of strain. Beyond this value, the lower quality cork produced high values of stress and a more pronounced slope approaching the densification stage, for the same strain values as the higher quality cork. Nevertheless, for applications that do not exceed 50% strain, the quality of the natural cork was irrelevant to its mechanical properties.

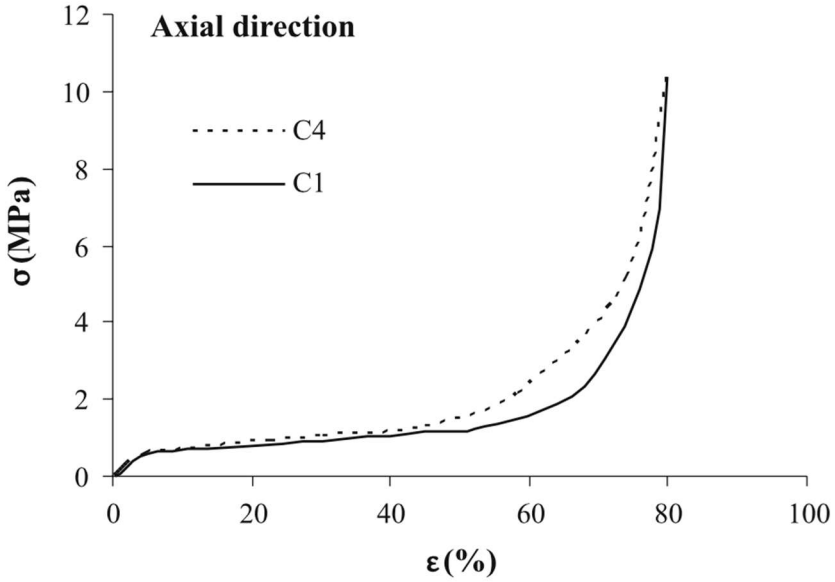

Figure 1.11: Influence that the quality of the natural cork has on its mechanical properties (C1-Good quality, C4-poor quality) [11].

When studying the influence of density on the properties of natural cork, the referred authors tested samples with different densities, between 121 and 197 kg/m^3 [11]. After the compression tests were performed, the Young's modulus values and the stress-strain curves were compared. The results showed that there was an increase in Young's modulus with the increase of density. Consequently, the values of stress on the plateau region are also higher for the denser cork. With the increase of the cork density, densification appears sooner and for lower values of strain.

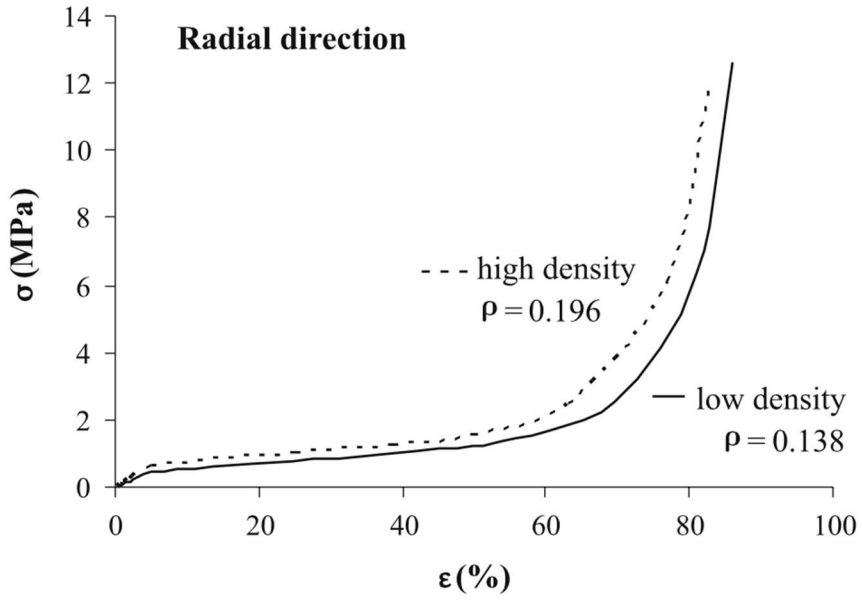

Figure 1.12: Influence that the density of the natural cork has on its mechanical properties (high density 0.196g/cm^3, low density 0.138g/cm^3) [11].

Another variable that may influence the mechanical response of the cork is the strain rate at which the material is compressed. To ascertain the influence of the strain rate on natural cork Rosa et al tested three different speeds of compression on cork samples cut from the same plank [10]. The results showed that the natural cork is strain rate dependent. The rate at which the material was compressed influenced the values of stress during the tests.

To evidence these influence these researchers, also performed an experiment on which the strain rate was altered during the test, and the resulting stress-strain curves showed a pronounced difference between the two rate of compression.

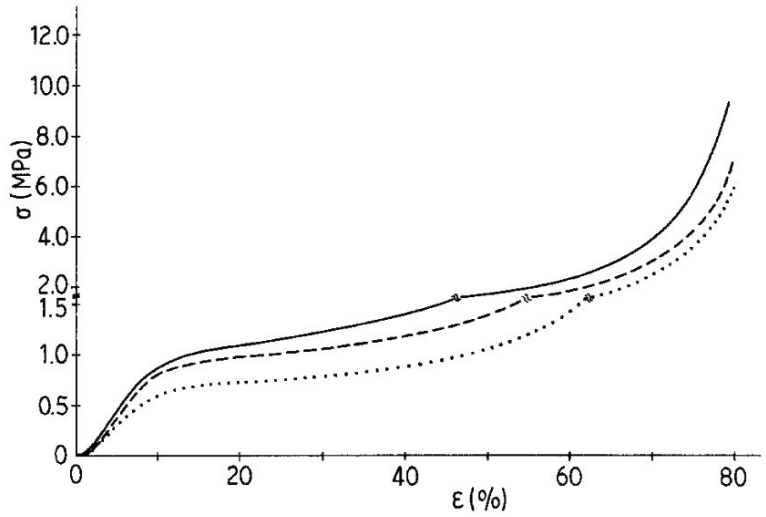

Figure 1.13: Effect of strain rate on the compression curve for the axial direction. [10].

1.3.5 Enhancing cork properties by addition of reinforcement materials

The use of reinforcement materials to enhance the final properties of the cork composite is a strategy that was already used in the past with great success. In the case of cork agglomerates, this possibility was already explored, using different strategies to enhance cork agglomerates properties [19].

Fernandes et al created a composite from a high density polyethylene filled with cork powder and coconut fibers[19]. The goal of their work was to improve the mechanical performance of the composite using as many natural materials as possible. With the addition of 10% of coconut fibers it was possible to increase the elastic modulus and tensile strength by 27% and 47% respectively, when compared with the unreinforced cork-based composite. Their results not only indicate that the addition of reinforcing material can be a feasible away to enhance the properties of cork-base composites but also help to complement a gap in the cork industry, regarding the cork waste.

1.4. Graphene based nanomaterials

Due to its outstanding properties, graphene (G) and graphene oxide (GO) are nowadays being used as functional additives, namely as mechanical reinforcement nanofillers in several polymer composites envisaging structural applications in aerospace, construction, and automotive sectors. The literature is full of good examples that corroborate this statement [20], [21]; [22].
In the following sub-sections, a brief description of these nanostructures, as well as their production and main properties, will be described.

1.4.1 Introduction to Graphene based nanomaterials

Carbon has many structures and properties ranging from sp^3 hybridized diamond to sp^2 hybridized graphite [23], [24].
Graphite is the most thermodynamically stable form of carbon at room temperature and has a layered and planar structure. In each layer, the carbon elements are distributed in a hexagonal lattice arrangement, with 0.142 nm of distance and the interlayer space is 0.335 nm [23]. Graphite is essentially made up of hundreds of thousands of layers of graphene (Figure 1.14).

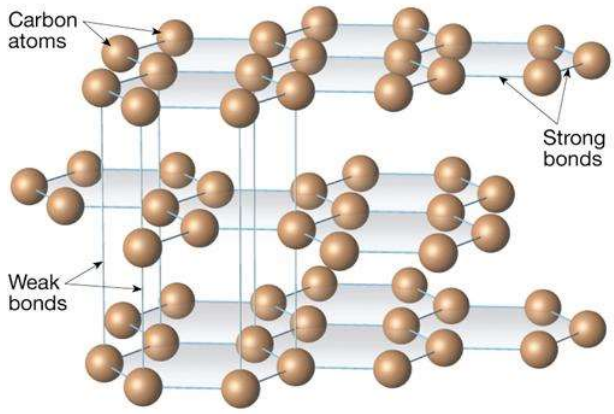

Figure 1.14: Schematic representation of the atomic structure of graphite.
(http://web.arc.losrios.edu/~borougt/GraphiteStructure.jpg).

In 2004, Novoselov and Geim were able to isolate one atomic layer from graphite crystal using an effective mechanical exfoliation with Scotch tape and then transferred this layer to a silicon substrate; they isolated for the first time a graphene nanosheet [25]. The joint award of the 2010 Physics Nobel Prize was attributed to these researchers, as stated by the Royal Swedish Academy (2010), "for groundbreaking experiments regarding the two-dimensional material graphene", highlights the

importance of this single atomic layer of carbon. This discovery is considered a breakthrough in the nanotechnology era, bringing the concept of single atomic component closer to reality.

Graphene is a one-atom-thick planar sheet of sp^2-bonded carbon atoms that are densely packed in a honeycomb crystal lattice (Figure 1.15 a and b). It possesses extraordinary physical properties, associated with its monolayer of covalently bonded carbon atoms [26] .

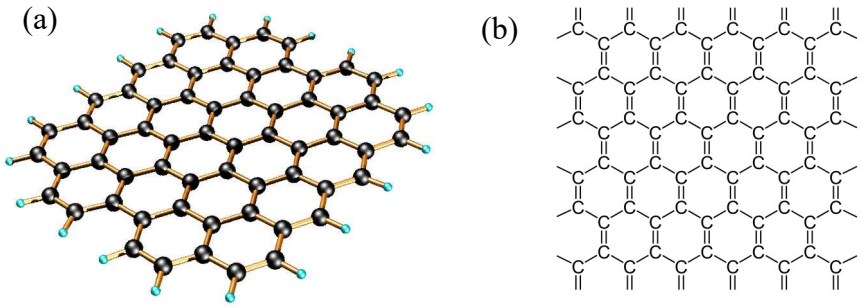

Figure 1.15: a) Idealized structure of a single graphene sheet and b) representation of the carbon bonding in the graphene lattice. (Both images are from internet images).

Graphene has displayed a variety of intriguing properties including high electron mobility at room temperature (250,000 cm^2/Vs) exceptional thermal conductivity (5000 W m-1 K-1) and superior mechanical properties with Young's modulus of 1TPa [27].

The synthesis of high quality graphene can be performed through various approaches, namely chemical vapor deposition, [28] [29] arc discharge [30] [31] and epitaxial growth in SiC. [32].

Graphene can also be prepared from the wet chemical exfoliation of graphite since graphite is in its self a series of billions of graphene layers stacked on top of each other. Graphite is a good source to obtain graphene since it is cheap and abundant. For that reason, it is suitable for the production of graphene on an industrial scale through mechanical or chemical exfoliation. The first refers to the single-layer sheets obtained by micromechanical cleavage techniques [33].

The second involves the chemical exfoliation with oxidative chemicals is accomplished due to the strength of interactions between water and the oxygen-containing (epoxide and hydroxyl) functionalities introduced into the basal plane during oxidation. The hydrophilicity leads water to readily intercalate between the sheets and disperse them as individuals. Mechanical stirring or sonication is employed to break the bonds between the carbon layers. The later allows for a faster and more effective cleavage, as the cavitation of bubbles generated by ultrasonic fields produces shock waves that break apart the graphite flakes. During this process, an intermediary form is

obtained: graphene oxide (GO). This intermediate specie obtained through these chemical methods is a planar carbon nanostructure with a high density of oxygen functional groups; that subsequently can be reduced into graphene typically by chemical [34] or thermal methods [35].

With a thermal treatment (deoxygenation) or a chemical reduction (for example using hydrazine), GO could be reduced to restore the graphene structure and its conductive properties. However, there are limitations, the chemical exfoliation does not allow an absolute control over the graphene layer number, also the quality of the GO 2D crystal framework tends to be lower than graphene, hindering its performance in several applications mainly in the electronic area. These defects in the crystalline network are mainly noticed in the chemical exfoliations due to ample surface modification. In addition, the ultrasonication method used for better exfoliation tends to create bigger structural damages in the GO [36].

Nevertheless, from the chemical point of view, the presence of oxygen functionalities at the GO surface may be very interesting because they provide reactive sites for chemical modification using known carbon surface chemistry [37]. GO is an atomic sheet of graphene decorated by several oxygenated functional groups (carboxylic, hydroxyl and epoxy) on its basal planes and at its edges, resulting in a hybrid structure comprising a mixture of sp^2 and sp^3 hybridized carbon atoms (Figure 1.16).

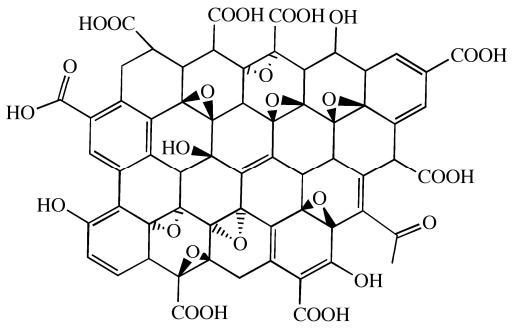

Figure 1.16: Graphene oxide molecular structure.

GO is an electrically insulating material due to the change in hybridization of the oxide carbon atoms from sp^2 to sp^3. As previously referred, through a process of reduction of the GO, it is possible to restore the electrical conductivity of GO, making it similar to pure graphene. For that reason, this is one of the most important reactions of GO [38] & [39]. Reduced graphene oxide (rGO) can be obtained by chemical or thermal reduction of the GO, where the material can recover the hybridized sp^2 configuration approaching of graphene configuration [40].

The thermal reduction has some advantages over the chemical one since it does not require the use of more chemicals, like those of the chemical reduction.

The incorporation of this nano-scaled material into the polymeric matrix is well documented either to confer or improve mechanical, thermal and fire-retardancy properties. Many studies reported that, even at low loading (between 0.5 and 5 wt.%), when incorporated in polymeric matrices, graphene and GO can strongly improve thermal, mechanical and fire-retardancy of the host polymer [41], [42] (see Table 2). For that, a good dispersion of the filler into the polymer matrix is crucial to overcoming the issues of interface that many times impairs the performance of these composites [43].

In the case of graphene, its hydrophobic character makes it prone to have a good dispersion in many polymers and organic solvents. On the other hand, as most of the polymers are hydrophobic and GO has a hydrophilic nature, it is necessary to modify/functionalize the polymer or/and the GO (by chemical or physical methods), to promote the good dispersion and chemical bonding [44], [45]. Generally, the incorporation of GO in materials results in high performance materials [46].

The discovery of graphene and its derivatives as a nanofiller has opened a new dimension for the production lightweight, low cost, and high-performance composite materials for a range of applications (Mayhew & Prakash 2013).

1.4.2 Graphene and graphene oxide used as mechanical reinforcement

Polymeric materials are versatile and as such, they are used in a varied range of applications in several industries from aerospace to automobile and medical (namely orthopedic), due to being light and easy to process. Although despite all its advantages, polymeric materials exhibit disappointing mechanical properties, such as low elastic module and reduce mechanical resistance, when compare to metallic and ceramic materials.

One way to enhance the mechanical properties of polymeric composites is to incorporate high rigidity particles. The polymeric industry has done this for decades now. However, to achieve a relevant improvement in mechanical, thermal and electric properties of the polymeric composites it's necessary to use a high quantity of reinforcing material, around 40 to 60% of the weight of the polymer itself. On the other hand, the introduction of reinforcing materials can negatively impact other properties of the polymeric matrix, such as its processability and density, rendering it inappropriate for some applications [47].

Recently, the research into nanomaterials as made possible the creation of new polymeric composites with nanomaterials as reinforcement, leading to high performance composites, with low concentrations of reinforcement. A nanocomposite is a material with nanoparticles, on which at least one of his dimensions is on the nanometric scale, those nanoparticles are scattered on the polymeric

matrix. The interaction between the polymeric matrix and the nanoparticles gives superiors properties to the nanocomposites to those of conventional composites.

The combination of nanoparticles with a polymeric matrix is of the utmost interest to several industries since it can greatly increase the composite's mechanical properties, such as its rigidity, tenacity, mechanical resistance, all with a fairly low density increase. Furthermore, it can also enhance additional properties, such as the reduction of its thermal expansion coefficient, improvement of its electrical conductivity and the reduction of its permeability to gas.

Graphene has been considered of great interest to the production of polymeric nanocomposites [39]. The production of GO from graphite and the reduction of the same through several processes aforementioned has made possible the production of affordable polymeric nanocomposites. Furthermore, in the case of nanocomposite material it might not be necessary to reduce the GO since the oxidized groups that protrude from the bidimensional plane of graphene can have a positive effect on binding the nanomaterial to the polymeric matrix.

The incorporation of GO or in some cases functionalized GO (to improve the compatibility between the matrix and the filler) in epoxy (EP) [48]–[52], polyethylene succinate (PES) [53][20], polystyrene (PS)[21] and polyurethane (PU) [22] [54] matrices were studied. In some cases, the results showed great enhancements in mechanical properties. Examples of these results are summarized in Table 1.

The incorporation of graphene into polymer matrix was also reported, for example in PU and Polyvinyl alcohol (PVA) composites [55]. The use of graphene and or GO extends to other type of materials beyond polymeric; they are being used in metals and ceramics as well. The incorporation of graphene on an aluminum matrix was also studied by [56]. The results demonstrated that a composite with 0.3wt.% of graphene reinforcement exhibited a 62% increase in tensile strength over the unreinforced matrix.

Also, graphene and GO are being used in polymer cellular materials providing to the final product superior physical and mechanical properties [57] [58].

Supercritical CO_2 method was employed to prepare GO reinforced foams, for example, phenolic/GO[59], PPC/GO[60] and PMMA/GO[61] foams and the mechanical properties were evaluated. The incorporation of 1 wt.% of GO in PPC foam resulted in a huge enhancement in compressive yield strength (670%) while the loading of 1.5 wt.% of GO in PMMA foam showed an improvement of 200% in compressive strength compared with neat foam material. The incorporation of graphene in EP foams was studied by Zegeye et al.[62]. Results indicated that the compressive and tensile modulus of the epoxy-based syntactic foams were significantly improved using 0.3 vol.% of filling fraction of graphene. Recently, Wicklein and others[58] prepared a novel fire-retardant and insulating foam material by freeze-casting of suspensions of cellulose nanofibres, GO, boric acid and

sepiolite nanorods. The results showed an improvement in compressive modulus. Some of these results are summarized in Table 1.

Table 1: Examples of polymer composites mechanically reinforced with GO and graphene.

Reinforcement	Material	GO concentration	Property	Enhancement (%)	Reference
GO	EP	GO 1.5 vol. %	tensile strength	85	[48]
	PES	GO 1.5 vol. %	tensile strength	45	[53]
	EP	GO 0.1 wt. %	tensile strength	20	[49]
	PS	GO-OPP 1 wt. %	tensile strength	25	[21]
	PU	GO 0.4 wt. %	elongation at break	132	[54]
	EP	GO 4 wt. %	compressive strength	33.5	[51]
	WPU	rGO 2 wt. %	tensile strength	750	[22]
	PES	GO 1 wt. %	tensile strength	81	[20]
	PPC foam	GO 1 wt. %	Compressive strength	670	[60]
	PMMA foam	GO 1.5 wt. %	Compressive strength	200	[61]
	PVA	G 1.8 vol. %	tensile strength	150	[63]
	TPU	G 5.1 vol. %	Elastic modulus	200	[64]
Graphene	Aluminium	G 0.3wt.%	tensile strength	62	[56]

Note (Abbreviations): EP – Epoxy; PES – Poly ethylene succinate; PS – Polystyrene; PU – Polyurethanes; PMMA – Poly(methyl methacrylate); PVA – Polyvinyl alcohol; TPU – Thermoplastic polyurethane; G – Graphene; GO-OPP – organophosphorus oligomer modified GO.

1.4.3 Graphene and graphene oxide used as fire retardant

As mentioned above, besides mechanical reinforcement, carbon-based nano additives hold great potential as exceptional nanoscale materials providing an attractive class of nanoparticle to be examined for flame retardancy of several polymers[65], [66], since polymers present high flammability that limits their application. Depending on the field of application, materials need to be submitted to tests to evaluate their response in a case fire situation. The fire-retardancy performance of polymers is usually evaluated by UL 94 (vertical and horizontal) burner test, LOI (limiting oxygen index) and cone calorimetry[67].

Cone calorimetry is one of the most complete tests in predicting fire-retardancy behavior, providing simultaneously quantitative data and also qualitative visual information. The fire properties that can be collected from the data include peak heat release rate, PHRR, total heat release, THR, heat release rate, HRR, among others[67]–[69]. It is expected that with the addition of flame-retardants, these parameters decrease.

Several studies were carried out to determine the potential of carbon-based nano additives on the fire resistance properties of several polymers [65], [66]. Those studies proved that the addition of nanoscale carbon-based materials on polymeric matrix has a measurable effect on its fire resistance. For instance, the incorporation of carbon nanotubes, CNTs, were reported to improve fire-retardancy [70]–[74]. More recently the incorporation of graphene and GO, also showed to have a positive effect on the fire retardant properties of polymers [58], [75]–[77]. Even the addition of small quantities of nanofillers (between 0.5 and 10 wt.%), was proved to have a noticeable impact on the fire-retardancy of the host polymer[42], [65], [78]–[80].

The flame-retarding behaviour of GO can be attributed to its ability to form a continuous, protective char layer that acts as a thermal insulator and a mass transport barrier [77], [81]. The presence of carbon nanofillers promotes the flame resistance by decreasing the release rate of combustible gasses and by creating an insulation protective layer on the surface of the polymer composite[82], [77], [81].

When the addition of carbon-based materials is not enough to meet the requirements of a certain application, two approaches have been attempted. In one of the cases, in addition of the carbon-based nanofillers, it is also added a traditional fire retardant agent (IFRs), taking advantage of the synergetic effect of both compounds. This addition is done directly during the mixing process.

Another approach is to functionalized carbon nanostructures with conventional flame retardants and then incorporated it on the polymeric matrix[83]–[85].

In this case, a better dispersion of the fillers in the matrix can be achieved and thus the fire-retardancy can be improved. Some examples are reported in Table 2.

Table 2: Examples of fire-retardancy improvement in polymer/graphene nanocomposites.

Polymer matrix	Filler	Concentration wt.%	Decrease (%)		Reference
			PHRR	THR	
EP	GO	1	10	40	[79]
PLA	Graphene	2	40		[86]
Functionalized GO					
PE	GO HGO GO HGO	1 1 3 3	8 28 9 29	3 -2 2 -6	[87]
PS	GO-AEPZ GO GO	0.5 1 2	19 26 39	5 9 14	[88]
PP	GO GO-MA	2	6 29	-7 3	[89]
PS	GO GO-OPP	5	21 34	3 5	[21]
EVA	rGO rGO-PPSPB	1	31 46	14 22	[90]
EP	GO GO-NS	1	16 23	6 6	[52]

Note (Abbreviations): EVA – Poly(ethylene-co-vinyl acetate); PE – Polyethylene; PLA – Polylactic acid; PP – Polypropylene; OPP – organophosphorus oligomer; NS–Nanosilica; HGO – N-aminoethyl piperazine and di(acryloyloxyethyl)methylphosphonate modified GO; GO-AEPZ – hyper-branched flame retardant based on N-aminoethyl piperazine and phosphonate derivative modified GO; GO-MA – melamine modified GO; rGO-PPSPB – poly(piperazine spirocyclic pentaerythritol bisphosphonate) modified GO; GO-NS – nanosilica modified GO

Chapter 2
Materials and methods

2.1 Materials

Cork grains were supplied by Amorim Revestimentos S.A. in two different particle sizes: 0.5-1mm (small grains) and 2-4mm, from now on referred as small and large grains, as shown in Figure 2.1.

Small Grain (0.5 to 1mm)	Large Grain (3 to 4mm)
	

Figure 2.1: Photographs of the cork grains.

Three different binders were provided by Flexpur (Ovar, Portugal) designated by flexible, intermediate and hard (Figure 2.2). This designation is associated with the physical and chemical characteristics that will determine the strength of agglomerate and therefore its application.

Flexible binder	Intermediate binder	Hard binder
		

Figure 2.2: Photographs of the three binders used in the present work.

The Flexpur Company did not provide technical information about the chemical composition of these binders. However, this company is known for producing polyurethane based products. Polyurethane polymers are traditionally and most commonly formed by reacting a di- or polyisocyanate with a polyol. Both the isocyanates and polyols used to make polyurethanes contain, on average, two or more functional groups per molecule. The Flexpur Company also refer that these binders are based on the most commonly used isocyanates are the aromatic diisocyanates, toluene diisocyanate (TDI) and methylene diphenyl diisocyanate, MDI (Figure 2.3).

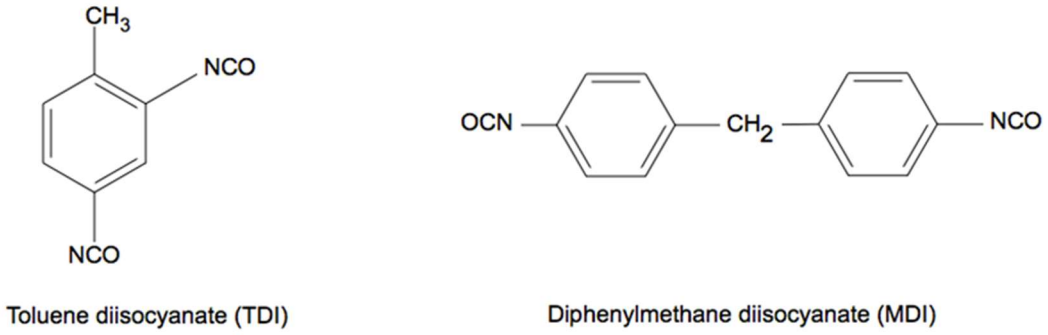

Figure 2.3: TDI and MDI molecular structure.

These pre-polymers have terminal isocyanate groups, NCO, which are highly reactive and could react with alcohol, amines and even with water. The general structure of the pre-polymer is represented in Figure 2.4. The crosslinking of these diisocyanate pre-polymers may also occur in contact with ambient moisture at room temperature (22 ºC) or high temperature allowing producing a solid.

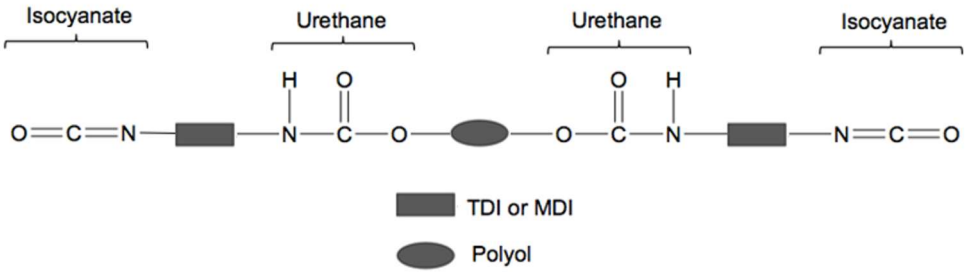

Figure 2.4: The structure of the pre-polymer

In the case of the agglomerated cork, the curing method affects the final properties of the material. Depending on the nature and grain size of the ground material, it is possible to obtain a large number of products for varied applications.

Usually, MDI leads to more rigid materials, while TDI is associated with flexible materials, because of the number of aromatic rings present in the isocyanate.

To verify the previous statements relating to the binder's compositions, Fourier Transform Infrared Spectroscopy - Attenuated Total Reflectance, FTIR-ATR was used to assess the chemical composition of the different binders. The infrared spectra were collected on a (Bruker Tensor 27) FTIR spectrophotometer. The spectra were obtained using an ATR tool in the range 500 to 4000 cm^{-1} at a resolution of 4 cm^{-1} and 256 scans per spectrum (Figure 2.5).

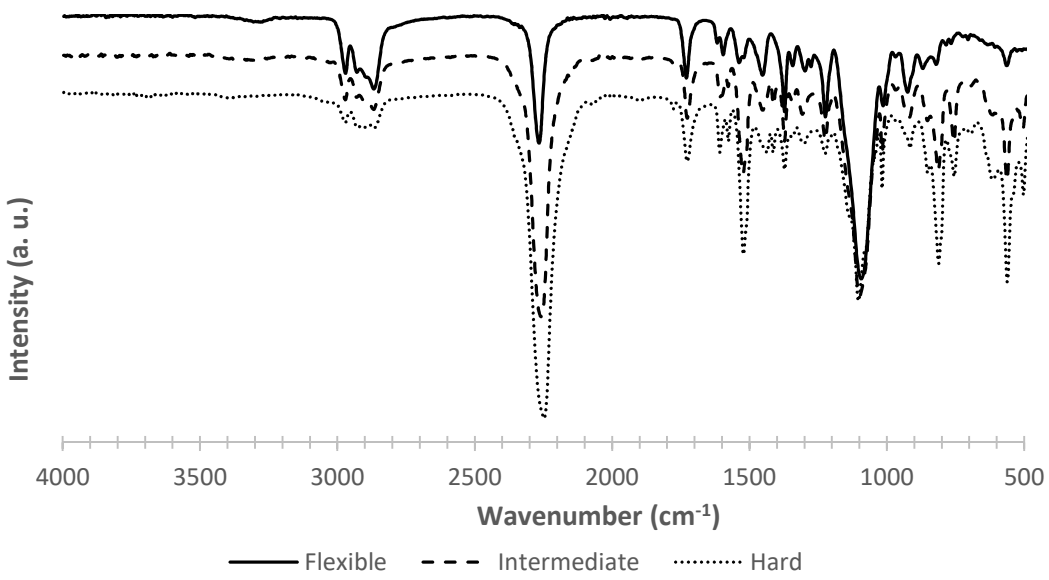

Figure 2.5: Transform Infrared Spectroscopy.

ATR-FTIR spectra of the different binder samples showed similar chemical composition, suggesting that the diisocyanate pre-polymers have almost the same composition, with the main variation in the amount of the chemical groups.

The stretching band corresponding to the isocyanate group (NCO) at 2250 cm^{-1} is sharper and stronger for the hard binder, indicating that the hard binder has a higher quantity of reactive groups. The peak groups at 2950, and 2875 cm^{-1} are attributed to the presence of alkanes with C-H stretch and are also present in all samples.

The sharp absorption peaks around 1730-1700 cm^{-1} correspond to the stretching vibration of esters C=O. The two peaks at 1523.76 and 1419.61 cm^{-1} show aromatic nitro compounds with specific bond N-O as in the structures of MDI or TDI cyanate group attached to the aromatic ring. The 1220 cm^{-1}

absorption peak is caused by the vibration of C=C in the benzene ring, and several weak peaks near 900-700 cm^{-1} belong to out-of-plane bending vibration of C-H in the multi-substituted benzene ring. The strong peak at 1100 cm^{-1} is attributed to the ether bond C-O-C stretch.

Based on the ATR-FTIR analysis it is possible to conclude that most probably the binders are PU pre-polymers based on MDI and TDI segments with different amounts of each.

As it will be shown in the results section, the role of the binder type on the final mechanical properties of the agglomerate is noteworthy.

2.2 Sample production

To prepare the samples, the different components were weighted and then mixed using a low speed blender (Figure 2.6). First, water was added to the cork and then the binder agent. To facilitate the addition of the agglomerating agent and minimize its waste a syringe was employed.

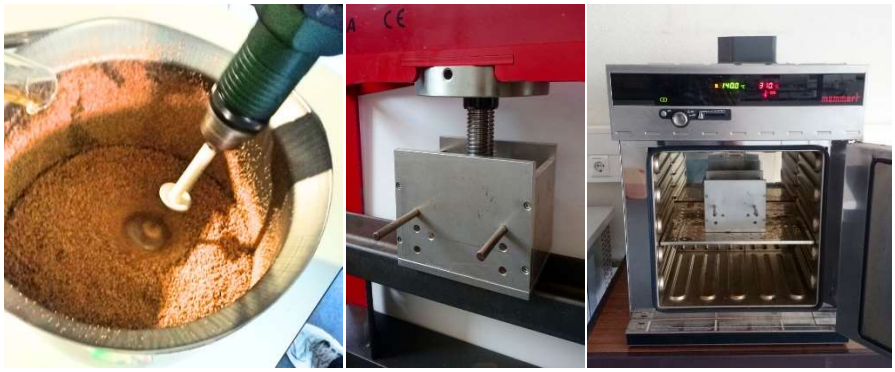

Figure 2.6: Sample production process.

After all the components were mixed, the material was poured into a mould to be compressed. Still, in the mould, the material was heated to 140ºC during two hours to accelerate the polymeric curing process. A variety of different agglomerates were produced to evaluate the influence of the density, grain size, binder type and its quantity percentage on the resulting mechanical properties, Table 3.

Table 3: Design of Experiments.

Binder type	Binder (wt.%)	Density(kg/m^3)	Grain Size
Flexible	15	200	Small(0.5-1mm)
Intermediate	15	200	Small(0.5-1mm)
Hard	15	200	Small(0.5-1mm)
Flexible	5	200	Small(0.5-1mm)
Flexible	10	200	Small(0.5-1mm)
Flexible	10	120	Small(0.5-1mm)
Flexible	10	160	Small(0.5-1mm)
Flexible	10	200	Large(2-4mm)

Chapter 3

Experimental Campaign

To determine the influence of the variables in study on the cork agglomerate mechanical response, several tests quasi-static and dynamic tests were performed. For a given test, one parameter was varied keeping the remaining fixed, for the sake of proper comparisons. For example, to examine the influence of the agglomerating agent used, all samples were produced with the same density, type of grain and percentage of binding agent. To assess the effect of density, grain size, binder type and quantity were fixed.

Regarding the mechanical properties, this study focused on properties like energy density, stress plateaus and densification strain for quasi-static tests and acceleration peaks, rebound energy and degradation after the second impact on dynamic tests. To ensure repeatability at least 3 tests were carried out for each different test.

3.1 Uniaxial quasi-static compression tests

Uniaxial quasi-static compressive tests were carried out using a Shimadzu AG50 KN testing machine. The uniaxial compression test proceeded up until the agglomerated cork densification stage. The samples were 50x50x50 mm cubes.

These samples were carefully centred and compressed with a very low strain-rate (3×10^{-3} s^{-1}). The output force–displacement curves allowed computing the energy absorbed per volume (energy density) and stress– strain curves.

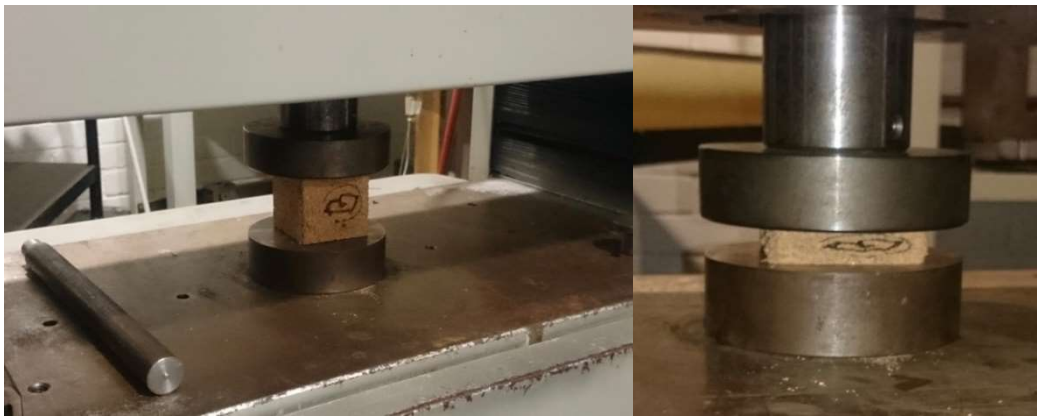

Figure 3.1: Compression test inicial and final point.

Figure 3.2 to Figure 3.6 presents stress–strain curves and energy density iso-curves for the variety of scenarios studied. Common to all cases, and as expected, a typical cellular material response is followed, where for a small uniaxial strain, there is a modest increase of stress, corresponding to the elastic stage. Then the materials exhibit a plateau for a wide deformation range from 5–60% keeping small stress values (depending on the sample). The ability to deform under nearly constant stress values is the reason why cellular materials are popular for applications where energy absorption is needed. Finally, the materials reach densification. Here an accentuated increase of stress occurs for small strain variations, which is usually denoted as the densification phase.

3.1.1 Binder Influence

As referred in chapter 2, three distinct binders were used. They were denoted as hard (MDI based), intermediate and flexible (TDI). Usually, MDI-based pre-polymers present a denser crosslinked structure, with a reduced molecular mobility of chains, while TDI-based pre-polymers have long flexible chains that allows the material extend with no rupture upon stretching [91]. When used to agglomerate cork, it was expected that each binder will confer these properties to the final composite. In this sense, the agglomerated cork prepared with the so-called hard binding agent will be characterized by higher Young modulus and earlier densification whereas the flexible will present lower Young modulus and later densification.

To test the influence of the binder type, several samples were prepared with exactly the same processing parameters the same type of grain, density (200kg/m^3) and percentage of the agglomerating agent (15 wt%) as depicted on Table 3. They were subjected to uniaxial compression and its stress-strain curves compared (Figure 3.2).

It is possible to infer a significant difference in the behaviour of the samples with different binder agents. It can be stated that the samples with the so-called intermediate and rigid binding agent have a higher Young's modulus resulting in a more pronounced stress plateau than the agglomerated cork with the flexible binding agent. This fact allows the two samples aforementioned to have a higher level of energy density for small strain values (10%). On terms of densification stage, a clear correlation can be derived: the harder the binder, the sooner densification will take place. A direct comparison between flexible and hard binders showed that for an energy density of 400kJ/m^3, both samples are at the onset of densification, but for different strain, where the flexible binder reaches densification for 70% strain against 50% for the hard binder.

Since the goal is to absorb large amounts of energy, the stress-strain curve should preferably include a long plateau with moderate stress values.

From this point of view, the samples with the intermediate and rigid binding agent are interesting because they exhibit a high plateau stress. Nevertheless, it reaches densification sooner than the

sample with the flexible binding agent, being the sample with the rigid binding agent the first to reach the densification stage. Also, the cork sample with the flexible binding agent has a longer plateau compared to the other two samples. Due to that fact, and although not being perfect, the sample with the flexible binding agent was used on the other subsequent tests performed.

It is then possible to conclude that the binder used has a significant impact on the properties of the final cork agglomerate when subjected to a quasi-static compression.

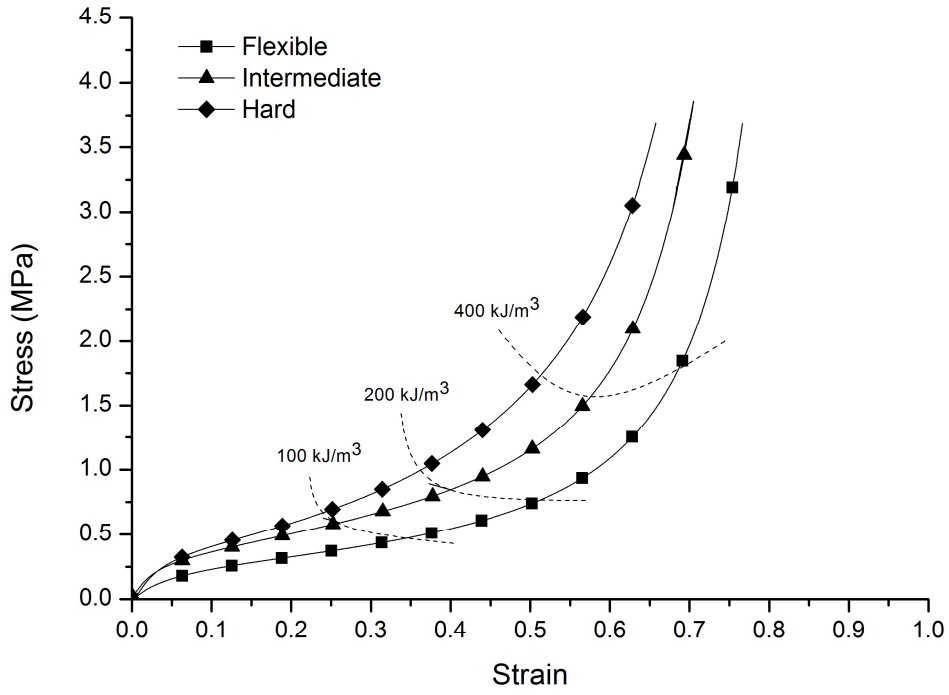

Figure 3.2: Influence of the agglomerating agent (same type of grain, density (200 kg/m^3) and 15 wt.% binding agent).

3.1.2 Binder Percentage Influence

On the second set of tests performed (Figure 3.3), the intention was to determine the influence of the percentage (wt.) of binding agent used. To this end, samples were prepared with the same type of grain, density (200 kg/m^3) and agglomerating agent (flexible binder), varying only the percentage of binding agent used (5, 10 and 15 wt.%). Iso-curves for energy density were calculated as well.
Samples with 5 and 10 wt.% present a very similar response under uniaxial compression. However, the 15 wt.% sample showed a lower stress plateau and reaches densification stage for higher strains. In this sense, it can be stated that increasing binder quantity (from 10 wt.% on), for the set of fixed parameters herein proposed, it will reduce Young modulus and consequently more deformation will be needed to absorb a given energy amount.

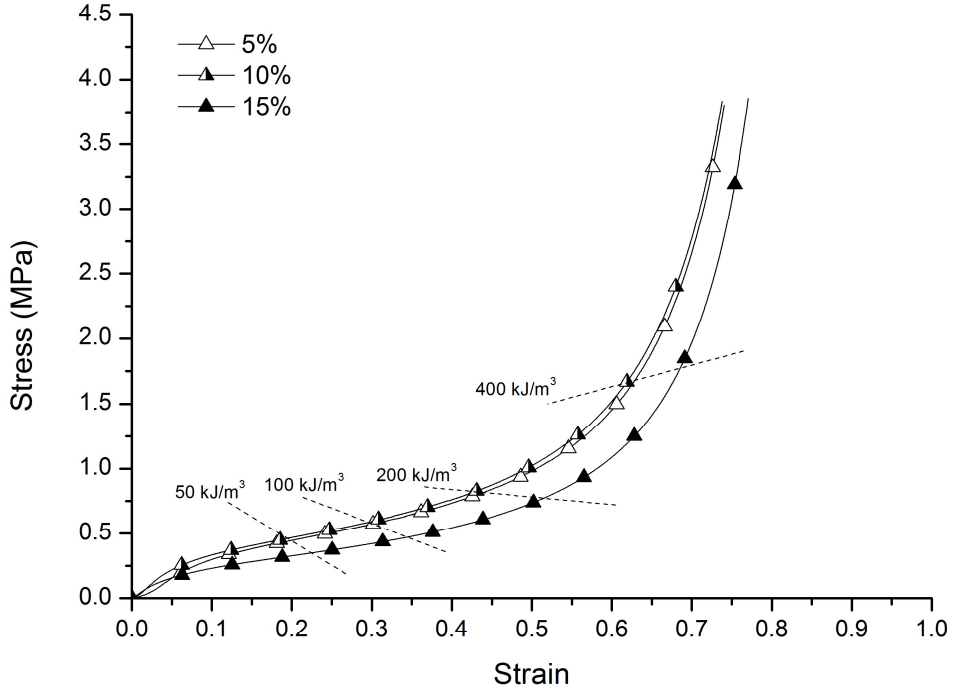

Figure 3.3: Influence of the percentage of agglomerating agent (same type of grain, density (200 kg/m^3) and flexible binder).

3.1.3 Density Influence

The third set of tests test performed (Figure 3.4), had the goal of determining the influence of the agglomerate density on the mechanical response. To that end, tree samples were prepared with the same type of grain (0.5-1mm), agglomerating agent (flexible binder) and agglomerating agent percentage (10 wt.%), varying only the density of the samples. Analyzing the results is possible to observe that the samples with higher density (200 kg/m^3) showed higher stress plateau and earlier densification stage.

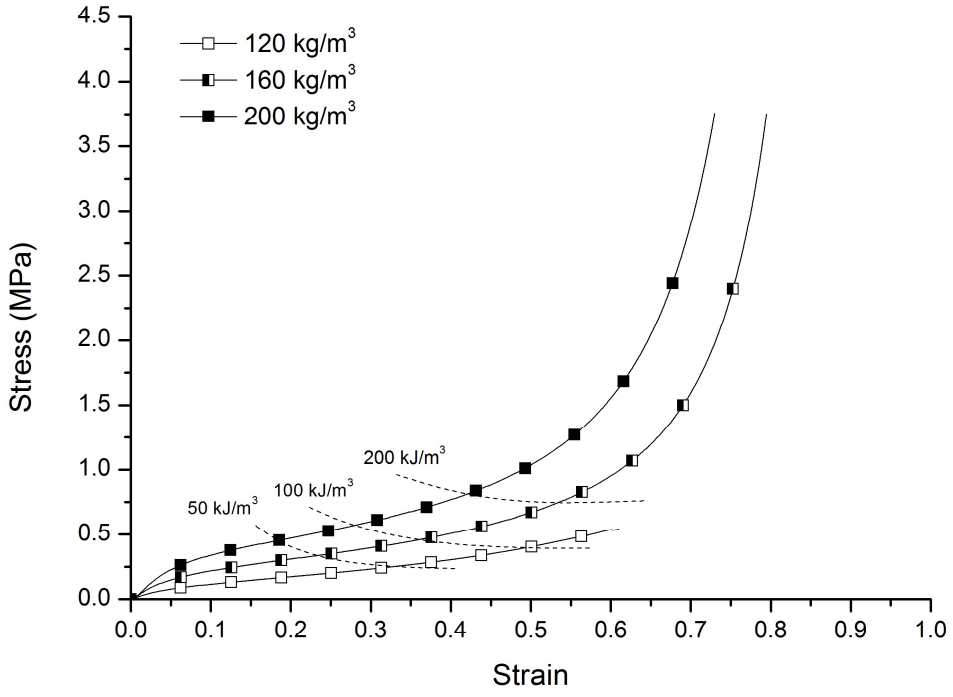

Figure 3.4: Influence of density (same type of grain and 10 wt.% of flexible binder).

The lightest sample (120 kg/m^3) showed the opposite trend but fails to keeps its structural integrity until the end of the test, collapsing at approximately 60% compressive strain (Figure 3.5). Finally, the 160 kg/m^3 keeps a good balance between structural integrity and mechanical response.

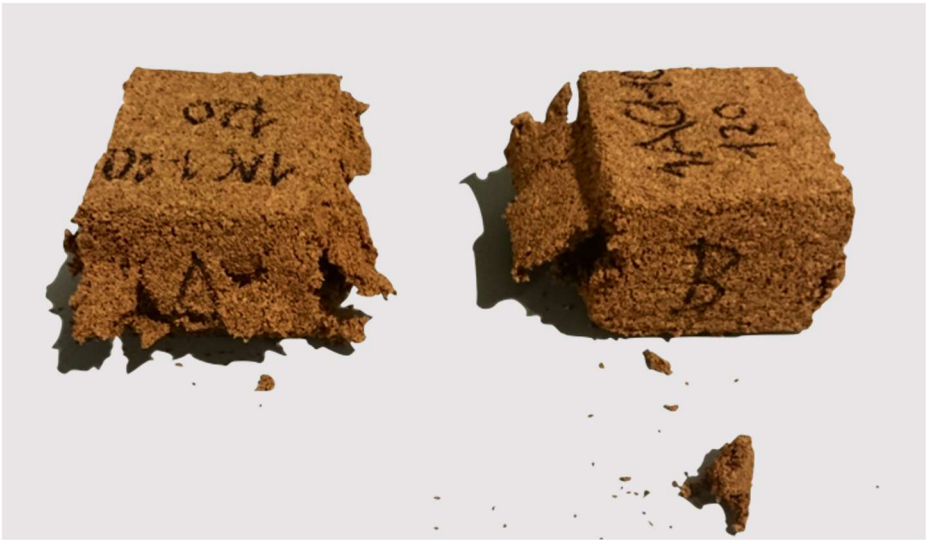

Figure 3.5: Cork agglomerate with a density of 120kg/m^3, collapsed after subjected to 60% compressive strain.

3.1.4 Grain Size Influence

In the final set of quasi-static compressive tests, the objective was to measure the influence of the cork grain size (Figure 3.6). For that goal, two types of samples were prepared with the same binding agent (flexible) binding agent percentage (10 wt.%) and density (200 kg/m^3), varying only the two grain sizes under study.

Analyzing the results, is possible to note that both samples have a similar behaviour. The sample with bigger grain has a slightly higher Young's modulus and plateau stress values, but also reach the densification stage sooner than the sample with a smaller grain. Such difference is probably due to a better dispersion of the agglomerating agent in the mixture.

After analysing these 4 sets of results, one can determine that grain size is the less determining factor in the overall final mechanical properties. However, grains of expanded cork can be bigger, up to 5mm, although not here studied.

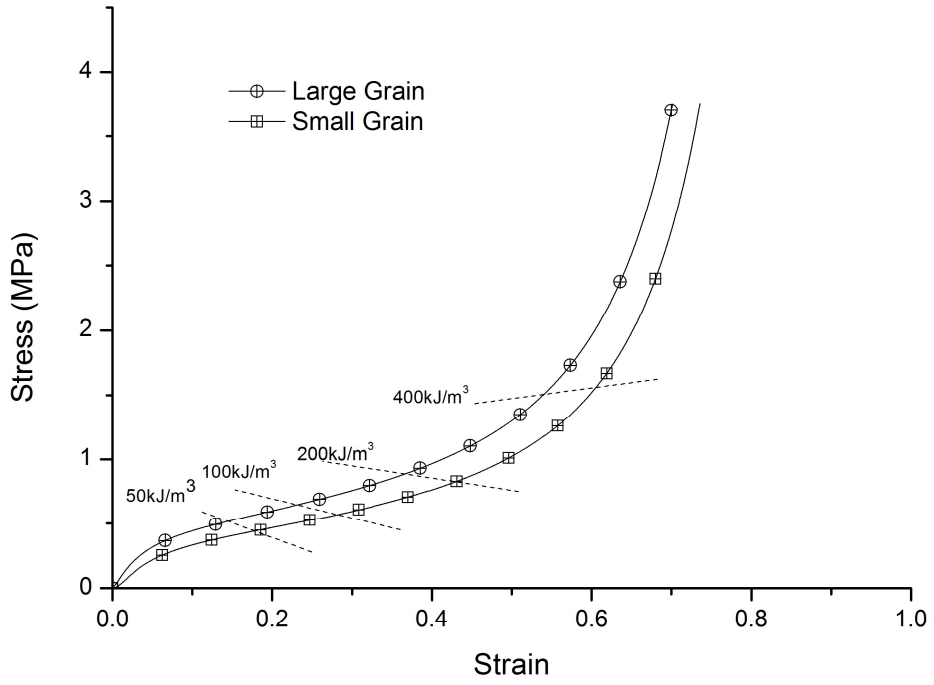

Figure 3.6: Influence of grain size (10 wt.% of flexible binding agent and density 200kg/m^3).

In what concerns the influence of binder, binder quantity, and agglomerate density, this study makes clear that mechanical properties can be easily tailored to a specific end. In short:

- To delay densification stage / lower stress plateau
    - Decrease agglomerate density
    - Use flexible, soft binder
    - Increase binder weight percentage
- To quicken densification stage / raise stress plateau
    - Increase agglomerate density
    - Use harder binder
    - Decrease binder weight percentage

Next session will evaluate the influence of the same set of variable but now under impact loading.

3.2 Impact tests

Impact tests were performed in a house-made, 3 meter high drop tower (
Figure **3.7**). A guided impactor is raised mechanically to 550mm, and then released reaching an average impact speed of 3.27 m/s, equivalent to an impact energy of 107.8 J. The flat impactor head dimensions are diameter 100 mm and weight 20 kg. In order to measure the acceleration history, force-displacement and stress-strain curves for all the samples, the load, position and time, obtained on the impact test, were acquired using a load cell of 5 kN and a position encoder. Data was synchronized and treated using Scilab. The samples dimensions were 50x50x50 mm. A second impact with the same energy was carried right after the first impact, in average with a 20-30sec time interval, the time needed to rise up the impactor again

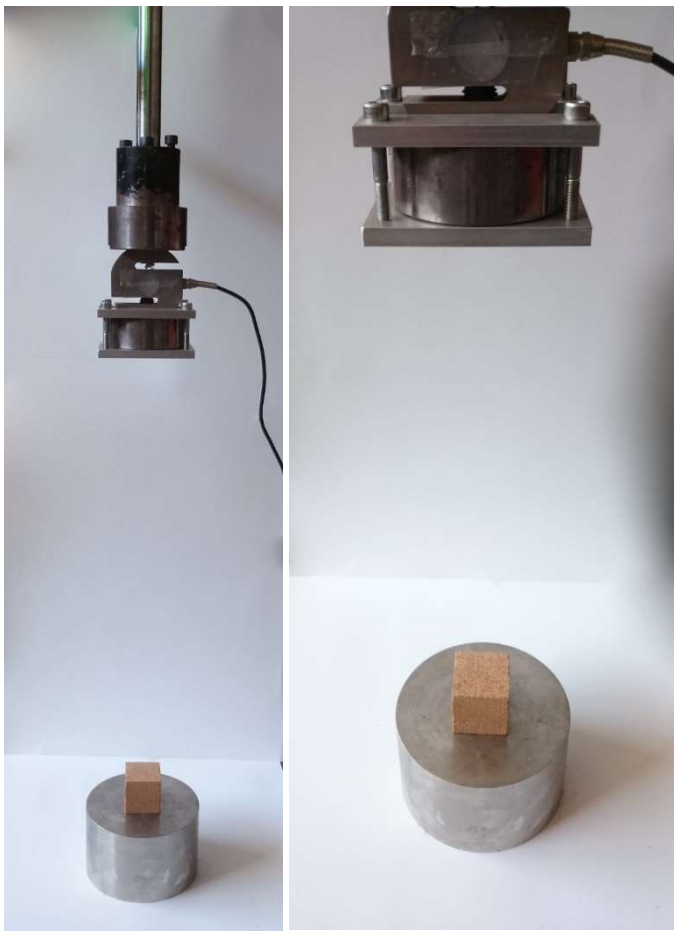

Figure 3.7: Dynamic tests setup.

Analogously to quasi-static tests, it is aimed to determine the influence of binder type and its weight percentage, grain size and its density - on the mechanical response of cork agglomerates, this time subjected to dynamic loading.

In addition, the degradation of mechanical response, due to damage, between a first and a second impact will be assessed to infer the material capability to handle multiple impacts. The following section will address the evaluation of energy densities, acceleration peaks, and stress-strain curves. In general terms, the outputs from a given test are summarized in Figure 3.8, comprising the impactor position and acceleration peak in function of time. For the sake of clearness, the full set of curves is only presented in the annex.

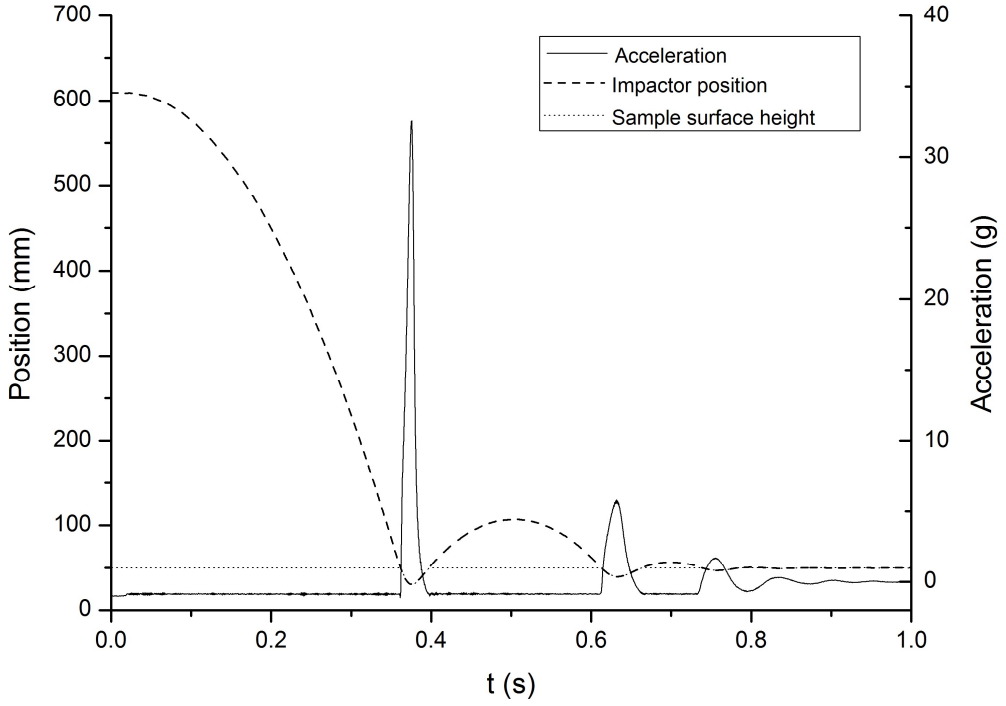

Figure 3.8: A typical set of data extracted from drop tower tests.

3.2.1 Stress-strain curves

Force-displacement curves allowed for the computation of stress-strain curves in the dynamic regime.

In the first set of tests (Figure 3.9) several samples of agglomerated cork with the same type of grain, density (200 kg/m^3) and percentage of the agglomerating agent (15 wt.%), were subjected to dynamic uniaxial compression. The binder type was changed to assess its effect. Stress-strain curves were computed, and peak values of acceleration registered as well.

It is possible to observe a significant difference in the stress-strain curves of the samples with different binder agents. Similarly, to quasi-static tests, (Figure 3.2), the intermediate and hard binding agents deliver a deformation plateau with higher stress and an earlier densification when compared to the flexible one. Regarding energy, harder binder agglomerates can store and dissipate higher values of energy for a less amount of strain, which results in lower acceleration peaks, even if such difference is less than 10%. This, the binder type has an effective impact on the properties of the final cork agglomerate under dynamic compression.

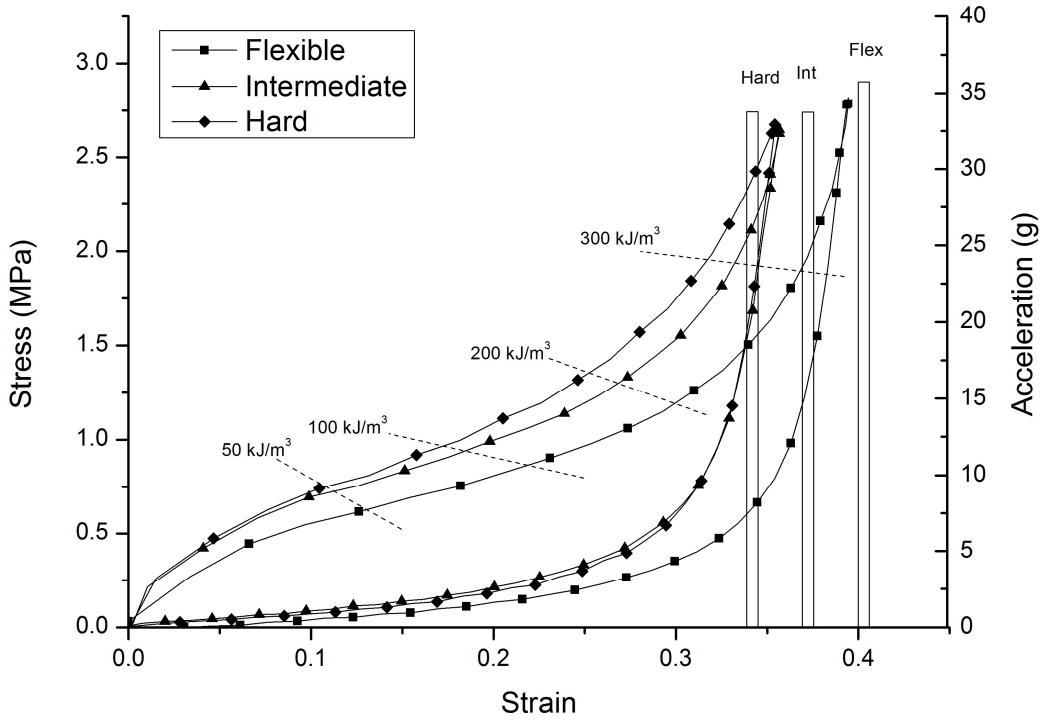

Figure 3.9: Influence of the agglomerating agent (same type of grain, density (200 kg/m^3) and 15 wt.% binding agent).

On the second set of dynamic tests performed (Figure 3.10), the intent was to determine the influence of the percentage (wt.%) of binding agent used. Three sets of samples were prepared with the same type of grain, density (200 kg/m^3) and agglomerating agent (flexible binder), varying only the percentage of binding agent used (5, 10 and 15 wt. %). A trend is observed in the sense that increasing binder percentage will lower the stress plateau and retard densification stage. The sample with a higher percentage of binding agent (15 wt.%) showed not only a lower stress plateau and later densification stages but also a higher peak acceleration for the energy impact under study. An important conclusion from these tests is that the amount of binder used should be tuned to an

optimum value, establishing a compromise between structural integrity (minimum value) but not obscuring the mechanical properties of the base cellular material (maximum bound).

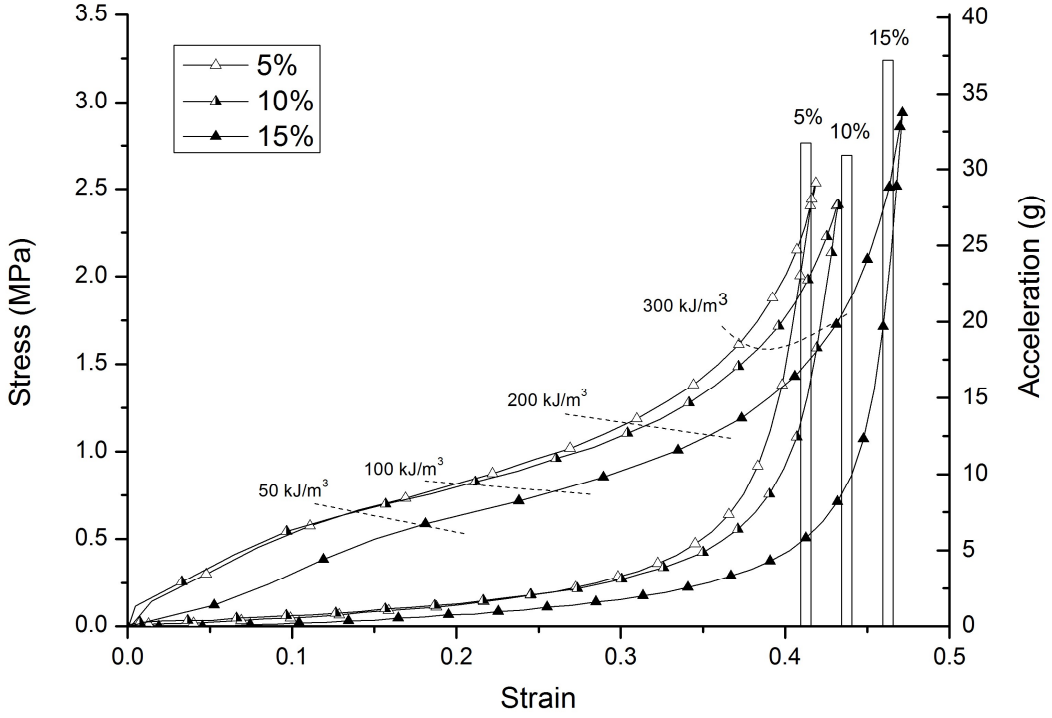

Figure 3.10: Influence of the percentage of agglomerating agent (same type of grain, density (200kg/m^3) and flexible binder).

The third set of dynamic tests was performed (Figure 3.11) to determine the agglomerated cork density influence. Three sets of samples were prepared with the same type of grain, agglomerating agent and agglomerating agent percentage (wt.%), varying only the density of the samples. Analysing the results is possible to observe that the mechanical behaviour of the three samples subjected to impact follows the same trend observed in quasi-static test tests (Figure 3.4). Increasing density values will raise stress plateau density and promote earlier densification. Samples of 120kg/m^3, the lightest herein studied, failed to keep its structural integrity during the impact tests, which makes clear the need of stablishing a minimum value for the agglomerate cork density for the sake of an acceptable structural integrity.

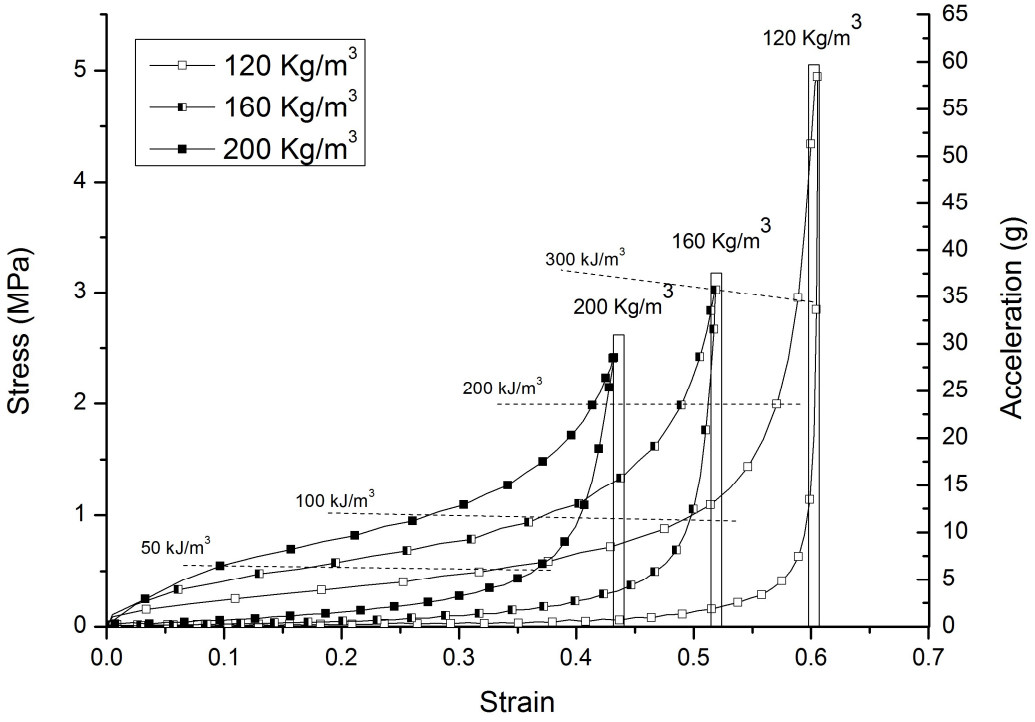

Figure 3.11: Influence of density (same type of grain and 10 wt.% of flexible binder).

On the fourth dynamic test, two samples were prepared with the same binding agent, binding agent percentage (wt.%) and density (200 kg/m^3), varying only the grain size of the samples, 0.5-1mm (small grain) and 3-4mm (large grain). Analysing the results is possible to notice an influence on stress plateau level and densification strain. Samples with smaller grain size showed later densification and lower stress plateau, possibly due to a better dispersion of the binding agent in the compound.

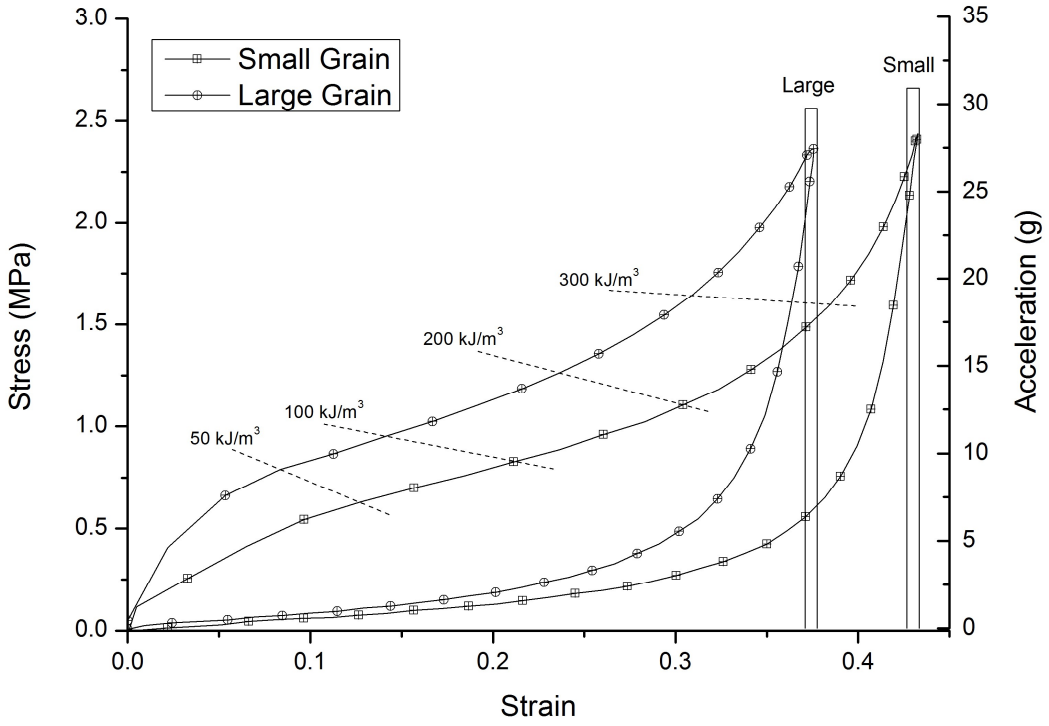

Figure 3.12: Influence of grain size (10 wt.% of flexible binding agent and density 200 kg/m^3).

The four sets of stress-strain curves herein presented make clear that the several processing parameters studied have significant influence also on the dynamic response of the agglomerates. There is also a clear agreement between the quasi-static and dynamic response of agglomerates regarding the influence of grain size, binder agents, and compound density.

The following sections focus on additional mechanical parameters that may be important assessing the viability of cellular materials for safety and multi-impact situations.

3.2.2 Acceleration Peaks

When cellular materials are used as liners for a safety device (e.g. helmets), the peak acceleration is correlated with the probability of sustained injuries. Likewise, if the material is used in packaging, smaller acceleration peaks will prevent more damage to the protected good.

Three sets of samples with three different agglomerating agents were impacted two times with the same energy (107 J), and their peak accelerations recorded and depicted in Figure 3.13.

As expected, all samples are damaged after the first impact. Consequently, the peak acceleration for the second impact will be naturally higher. The influence of the binding agent is clear. The sample with the flexible agglomerating agent presents the higher increase on peak acceleration upon the second impact. It is possible to note a gradual decrease in damage effects as increasing binder agent's rigidity. This is mostly due to a better capability of harder binders to keep the integrity of the agglomerate under extreme loadings.

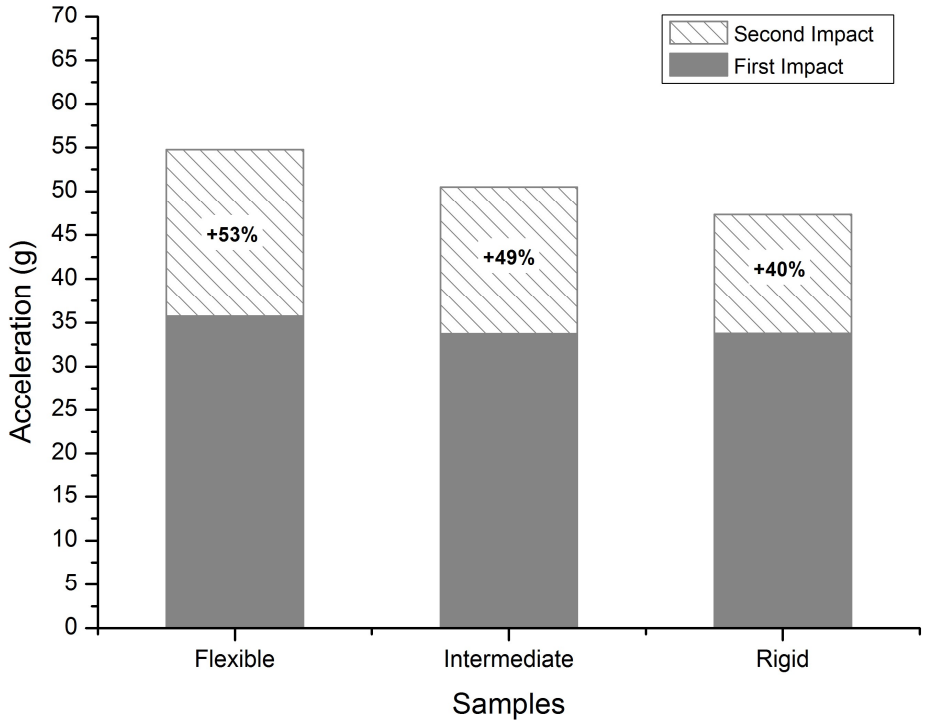

Figure 3.13: Influence of the agglomerating agent (same type of grain, density (200 kg/m^3) and 15 wt.% binding agent).

On the second phase of tests, this time fixing the binder type and compound density, three sets of samples with 5, 10 and 15 wt.% of agglomerating agents were tested, and their values of peak accelerations presented in Figure 3.14.

From Figure 3.14, it is possible to observe that the binding agent percentage used on the samples influences its response, but not in a linear way. In fact, and similarly to what was inferred from stress-strain curves (Figure 3.10), samples with 5 and 10 wt.% behave similarly, and only the 15 wt.% delivered higher values of peak acceleration for both impacts.

The relative increase of acceleration peak from the first to the second impact appears to be independent of binder quantity, which presented a different trend compared to binder type, as shown in the previous section.

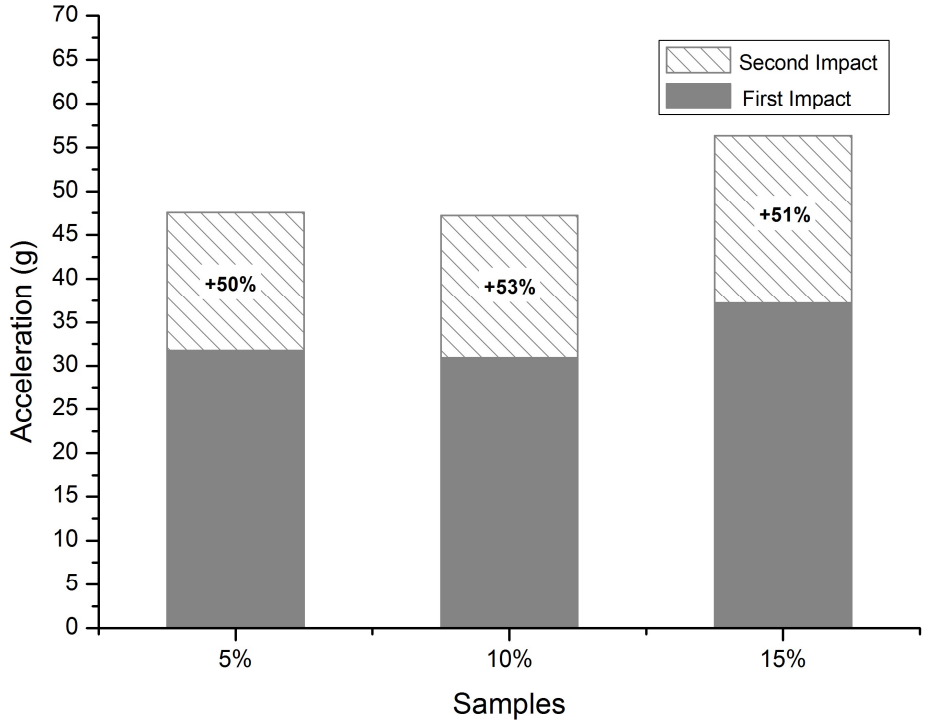

Figure 3.14: Influence of the percentage of agglomerating agent (same type of grain, density (200 kg/m^3) and flexible binder).

To test the influence that the sample density has on the values of acceleration, three sets of samples with three different densities were tested, keeping fixed binder type and binder quantity. The values of maximum acceleration for the two impacts are presented in Figure 3.15.

The sample with a density of 120 kg/m^3 was destroyed during the first impact, yielding the higher value of peak acceleration, and preventing the realization of a second impact. Regarding the 160 kg/m^3 and 200 kg/m^3 samples, it can be noticed a very significant degradation of crashworthiness properties for the first, while the second presents the lower peak values on both impacts. For the case in study, with an impact energy density of 800 kJ/m^3, the samples with 200 kg/m^3 is the best option. However, the pay-off is a higher weight. In this sense, for lower impact energy densities a lighter compound may be chosen as well.

So, as an empirical rule, one could choose a compound density that is a quarter than the impact energy density to be sustained. Naturally, changing binder and quantity may affect these results as well.

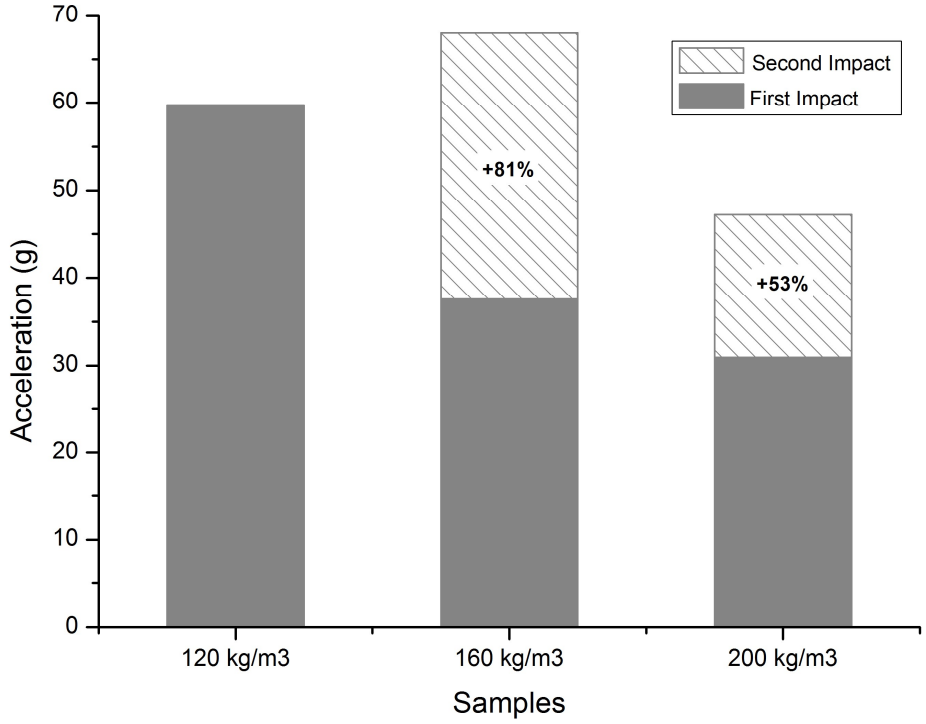

Figure 3.15: Influence of density (same type of grain and 10 wt.% of flexible binder).

Finally, a final set of tests was carried out changing only grain size, but keeping binder, quantity and sample size fixed. For the density of 200 kg/m^3, grain size played a marginal role, yielding just a higher peak acceleration on the second impact for the samples with higher grain size. A bigger damage after the first impact is probably due to the worst dispersion of binder in the compound due to a larger grain size.

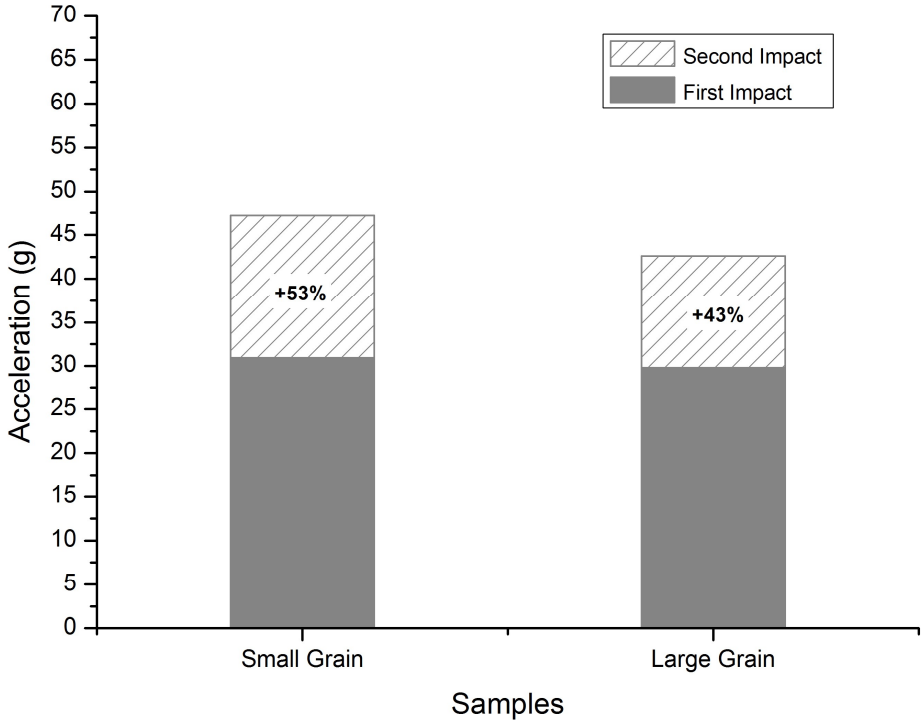

Figure 3.16: Influence of grain size (10 wt.% of flexible binding agent and density 200kg/m^3).

3.2.3 Bounce back

One should recall that one interesting property of cork agglomerates is exactly the capacity to recover its dimensions after deformation, given its viscoelastic properties. The percentage of impact energy returned to the impactor right after impact is also evaluated, and from now on denoted as a bounce-back effect. For safety devices, it is undesirable that a significant amount of impact energy return to its load source. So, a compromise between absorbed and returned energy must be kept for devices sustaining multiple impacts.

In the following graphs, the bounce back measurement is measured in percentage and quantifies the amount of energy that was not absorbed by the samples but returned to the impactor, making it

bounce back and recover potential gravity energy. Influence of binding agent, the percentage of binding agent, the density of the samples, and the size of the cork's grain used have on the samples' were assessed and depicted in Figure 3.17 to
Figure 3.20.

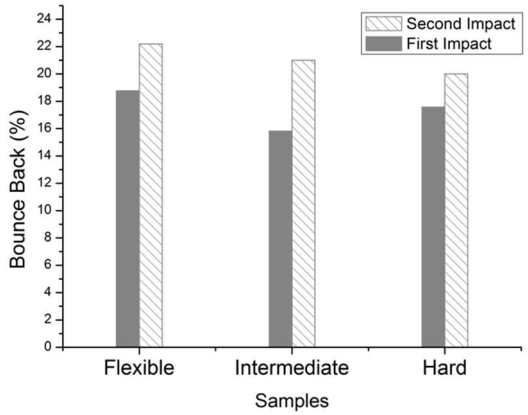

Figure 3.17: Influence of the agglomerating agent (same type of grain, density (200kg/m^3) and 15 wt.% binding agent).

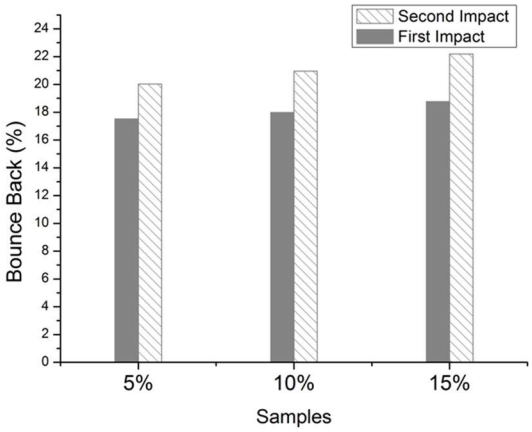

Figure 3.18: Influence of the percentage of agglomerating agent (same type of grain, density (200kg/m^3) and flexible binder).

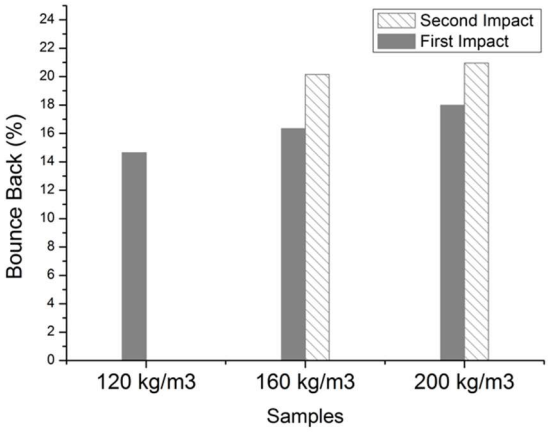

Figure 3.19: Influence of density (same type of grain and 10 wt.% of flexible binder).

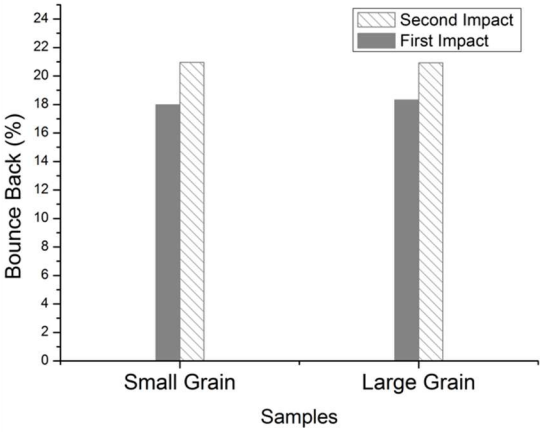

Figure 3.20: Influence of grain size (10 wt.% of flexible binding agent and density 200kg/m^3).

Table 4: Bounce back values

Naturally, for all samples tested the value of bounce back increases from the first impact to the second impact. Indeed, even if cork grains keep the crashworthiness and elastic properties after several impacts, the same cannot be stated for the polyurethane binders, that absorbs energy plastically.

Moreover, subsequent impacts will present fewer amounts of energy absorbed through plastic deformation and less energy dissipated thorough micro cracks generated in the cork grains/binder interfaces. A larger amount of energy will be stored visco-elastically and released upon unloading. The influence of processing parameters is more noticeable for the second acceleration peaks and regarding binder agents and quantities.

3.3 Graphene reinforcement

3.3.1 Material and methods

To determine the influence of the introduction of graphene nanoplates (GNP) and graphene oxide (GO) on the agglomerated cork mechanical response, several tests quasi-static and dynamic tests were performed. For a given test, one parameter was varied keeping the remaining fixed, for the sake of proper comparisons. To examine the influence of the graphene reinforcement, all samples were produced with the same density, type of grain and percentage of binding agent.
Figure 3.21, display the seven different samples tested.

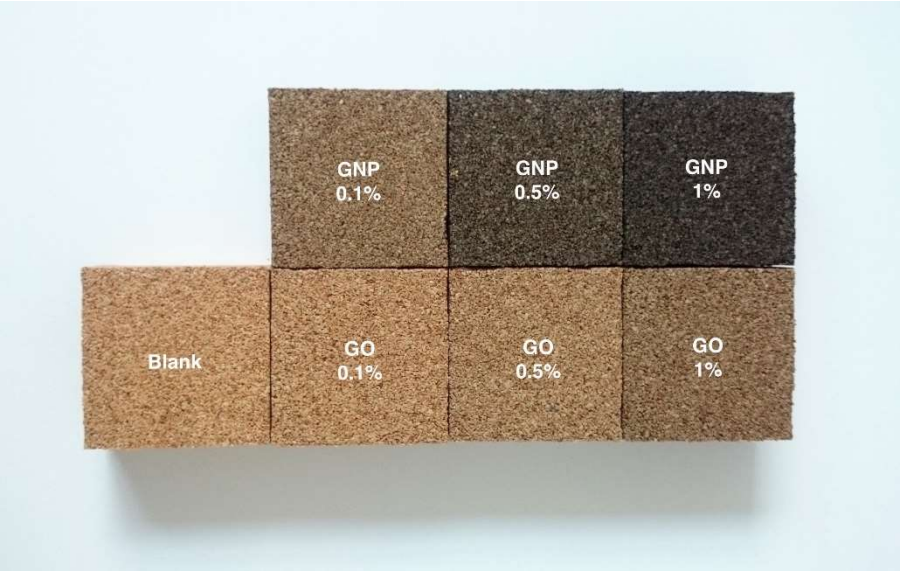

Figure 3.21: Seven different damples tested.

3.3.2 Uniaxial quasi-static compression tests

Uniaxial quasi-static compressive tests were carried out using a Shimadzu AG50 KN testing machine. The uniaxial compression test proceeded up until the agglomerated cork densification stage. The samples were 25x25x25 mm cubes.

These samples were carefully centred and compressed with a low strain-rate ($6{,}67 \times 10^{-3} s^{-1}$). The output force–displacement curves allowed computing the energy absorbed per volume (energy density) and stress– strain curves.

Three samples of agglomerated cork with the same binding agent (flexible), type of grain, density (150kg/m^3) and percentage of the agglomerating agent (10 wt.%), were tested. The only factor in study was the percentage of GNPs on the samples and its influence on the mechanical properties of the agglomerated cork. To that end, samples with 0.1, 0.5, 1 wt.% of GNPs were subjected to uniaxial compression and its stress-strain curves compared Figure 3.23.

Analyzing the Figure 3.23, it is possible to observe that the samples with 0.1% and 0.5% of GNPs present the same behaviour, with a small increase in stress values, from 30% onwards, compared to the sample without GNPs. The sample with 1 wt.% of GNPs presented higher values of stress, for values of strain superior to 30%, compared to all the other samples. Nevertheless, the addition of GNPs to the agglomerated cork does not affect the Young modulus of the agglomerated cork. One possible explanation for the small differences observed was the small quantity of GNPs used. Perhaps with the increase of GNPs percentage, the results would be different.

Graphene Nano Plates (GNPs)

Figure 3.22: Graphene Nano Plates.

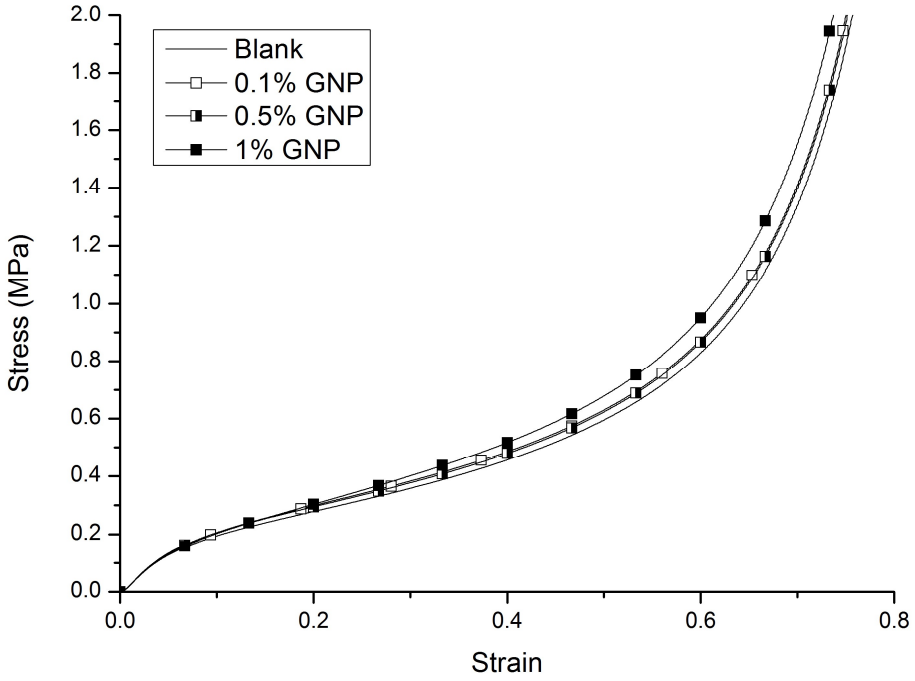

Figure 3.23: Influence of the GNP reinforcement (same type of grain, density (150kg/m^3) and 10 wt.% binding agent).

Graphene Oxide (GO)

Figure 3.24: Graphene Oxide

Similarly, to the test with GNPs, three samples of agglomerated cork with the same binding agent (flexible), type of grain, density (150 kg/m^3) and percentage of the agglomerating agent (10 wt.%), were tested. Varying only the percentage of GO on the samples and studying its influence on the mechanical properties of the agglomerated cork. The percentage of GO used was the same as the GNPs, 0.1, 0.5, and 1 wt.% Analyzing the stress-strain curves, it is possible to observe that the

samples with 0.1 and 0.5 wt.% of GO present the exact same behavior, as was the case with the samples with 0.1 and 0.5 wt.% of GNPs, with a small increase in stress values, from 30% strain onwards, compared to the sample without GO. The sample with 1 wt.% of GO presented a similar behaviour to the sample with no reinforcement. The increase of reinforcement from 0.1%, 0.5% to 1%, did not impact the properties of the sample.

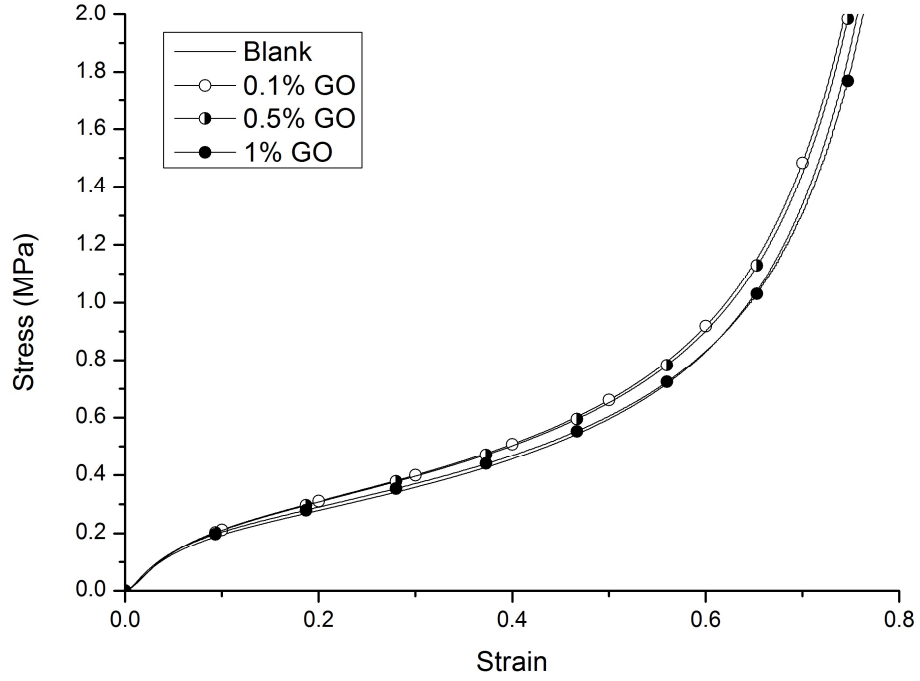

Figure 3.25: Influence of the GO reinforcement (same type of grain, density (150kg/m^3) and 10 wt.% binding agent).

This behaviour can be explained by carefully observing the sample exemplified in Figure 3.26, it is possible to notice some dark spots of GO, denoting that the dispersion of the nanophase was not well succeeded under the present experimental conditions. A good dispersion of the reinforcement agent is an important factor on how the reinforcement will impact the overall properties of the final material.

Figure 3.26: Graphene poorly dispersed.

3.3.3 Burn Test

In this test, seven samples of agglomerated cork with the same binding agent (flexible), type of grain (0.5 to 1mm), density (150 kg/m^3) and percentage of the agglomerating agent (10 wt.%), were tested. The only factor in study was the influence of the percentage of GNPs and GO on the samples resistance to fire. To that end, samples with 0.1, 0.5, and 1wt.% of GNPs and GO, as well as a blank sample with zero percent of reinforcement material, were subjected to a burn test.

This test was carried out using a lighter and a sample suspended by a wire (Figure 3.27). In this test a flame is applied to the bottom of the sample for 3 s, followed by a second application (3 s) if the specimen self-extinguishes.

Figure 3.27: Burning test vertical sample set-up (sample with small grain (0.5-1mm), density (150kg/m^3) and 10 wt.% of flexible binder agent)

During the burn test, it was possible to observe that the samples with nano fillers behaved differently from the blank sample. The samples with 1 wt.% of GO showed a slightly higher resistance to fire compared to the sample with no reinforcement. Nevertheless, when testing the samples with 0.1 and 0.5 wt.% of GO, no noticeable difference was observed.

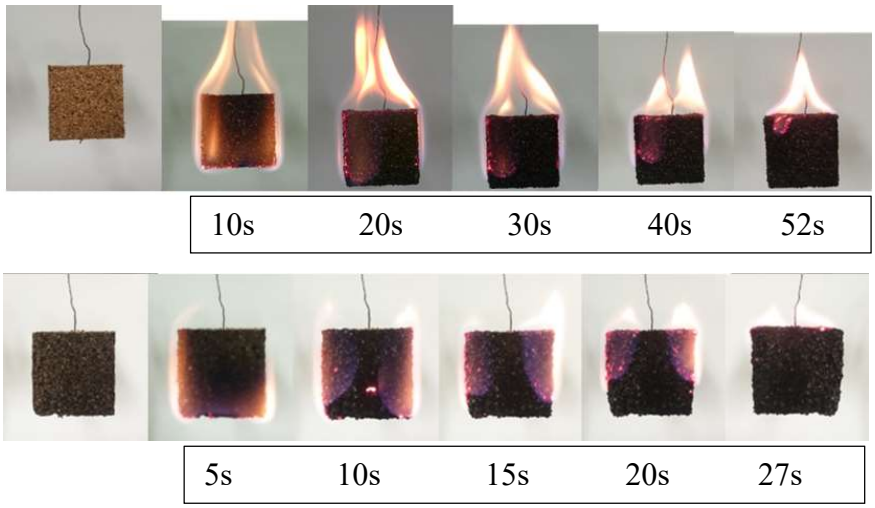

Figure 3.28: Comparison between the sample without reinforcement and the sample with 1 wt.% of GNP.

This can be attributed to the low amounts of nano fillers present in those samples and also to the low dispersion of the GO nano fillers in the agglomerated cork, as referred previously.

The incorporation of 0.1% and 0.5% of GNPs, caused a noticeable increase in the samples resistance to fire. Nonetheless, it was in the sample with 1 wt.% of GNPs that the influence of the graphene nano plates on the resistance to combustion of the agglomerated cork Figure 3.28 was more pronounced.

Chapter 4
Conclusions

This work establishes clear guidelines in what concerns processing of cork agglomerates. So far, in literature, agglomerate cork has been being used in a variety of applications, where specifications listed are given regarding density and grain size and as received from the manufacturers. Large cork companies have already the knowledge on how to tune up some mechanical properties, but such techniques are being kept secret to give commercial advantages.

This work shed light on many different processing parameters influencing the final mechanical properties of cork agglomerates. Type of binder, its weight percentage, grain size and agglomerate density were the parameters varied to test its significance on quasi-static and dynamic responses. As well as the influence of nano fillers reinforcements, like graphene and graphene oxide.

It becomes clear that a material designer can tailor up the mechanical response by changing, for instance, the binder type, delaying densification or promoting deformation larger stress plateaus. A huge window of possibilities now arises in what concerns the synthetization of new polymers with specific ends. In the same fashion, mechanical behaviour can be further tuned up by increasing binder quantity of playing with the quantity of cork grains, to raise the composite density. A lower bound should always be observed to keep the structural integrity of the material under loading. The upper bound is limited by the desired material weight.

Impact tests allowed to infer the influence of the referred processing parameters on the dynamic response of the material, in particular, its crashworthiness capabilities under single or multi-impact loading. For safety gear, this study allows developers to have an idea on how to change processing parameters to reduce peak accelerations, damage between impacts or optimize bounce back effects.

It is important to note that every specific material application involves different design requirements and different working loads. Doing so, the data herein presented must be read and adapted accordingly.

With the current urgency to promote sustainable materials to produce high quality goods, substituting their synthetic counterparts, this study aims to provide a comprehensive guide on how to choose cork agglomerates or tailor it up for specific needs.

The inclusion of the carbon nanostructures on the cork agglomerates needs to be optimized. The fire retardant properties were clearly observed. However, in order to improve the mechanical properties a methodology to better disperse the nanoadditives in the composite needs to be improved.

Bibliography

[1] I. Alcântara, F. Teixeira-Dias, and M. Paulino, "Cork composites for the absorption of impact energy," *Compos. Struct.*, vol. 95, pp. 16–27, 2013.

[2] M. Paulino and F. Teixeira-Dias, "An energy absorption performance index for cellular materials – development of a side-impact cork padding," *Int. J. Crashworthiness*, vol. 16, no. 2, pp. 135–153, 2011.

[3] L. J. Gibson and M. F. Ashby, "Cellular solids. Structure and properties." p. 502, 1997.

[4] R. J. A. de Sousa, D. Gonçalves, R. Coelho, and F. Teixeira-Dias, "Assessing the effectiveness of a natural cellular material used as safety padding material in motorcycle helmets," *Simulation*, vol. 88, no. 5, pp. 580–591, 2012.

[5] F. A. O. Fernandes and R. J. Alves De Sousa, "Motorcycle helmets - A state of the art review," *Accid. Anal. Prev.*, vol. 56, pp. 1–21, 2013.

[6] F. A. O. Fernandes, R. T. Jardin, A. B. Pereira, and R. J. Alves de Sousa, "Comparing the mechanical performance of synthetic and natural cellular materials," *Mater. Des.*, vol. 82, pp. 335–341, 2015.

[7] M. A. Fortes and M. Teresa Nogueira, "The poison effect in cork," *Mater. Sci. Eng. A*, vol. 122, no. 2, pp. 227–232, 1989.

[8] L. J. Gibson, K. E. Easterling, and M. F. Ashby, "The structure and mechanics of cork," *Proc. R. Soc. A Math. Phys. Eng. Sci.*, vol. 377, no. 1769, pp. 99–117, 1981.

[9] H. Pereira, J. Graça, and C. Baptista, "The effect of growth rate on the structure and compressive properties of cork," *IAWA Bull.*, vol. 13, pp. 389–396, 1992.

[10] M. E. Rosa and M. A. Fortes, "Rate effects on the compression and recovery of dimensions of cork," *J. Mater. Sci.*, vol. 23, no. 3, pp. 879–885, 1988.

[11] O. Anjos, H. Pereira, and M. E. Rosa, "Effect of quality, porosity and density on the compression properties of cork," *Holz als Roh - und Werkst.*, vol. 66, no. 4, pp. 295–301, 2008.

[12] M. F. Ashby, "The properties of foams and lattices," *Philos. Trans. R. Soc. A Math. Phys. Eng. Sci.*, vol. 364, no. 1838, pp. 15–30, 2006.

[13] S. P. Silva, M. A. Sabino, E. M. Fernandes, V. M. Correlo, L. F. Boesel, and R. L. Reis, "Cork: properties, capabilities and applications," *Int. Mater. Rev.*, vol. 50, no. 4, pp. 256–256, 2005.

[14] A. Costa, H. Pereira, and A. Oliveira, "Variability of radial growth in cork oak adult trees under cork production," *For. Ecol. Manage.*, vol. 175, no. 1–3, pp. 239–246, 2003.

[15] C. Fialho, F. Lopes, and H. Pereira, "The effect of cork removal on the radial growth and phenology of young cork oak trees," *For. Ecol. Manage.*, vol. 141, no. 3, pp. 251–258,

2001.

[16] R. T. Jardin, “Caracterização do comportamento mecânico em regime estático e dinâmico de aglomerados de cortiça,” 2014.

[17] R. T. Jardin, F. A. O. Fernandes, A. B. Pereira, and R. J. Alves de Sousa, “Static and dynamic mechanical response of different cork agglomerates,” *Mater. Des.*, vol. 68, pp. 121–126, 2015.

[18] H. Pereira and E. Ferreira, “Scanning electron microscopy observations of insulation cork agglomerates,” *Mater. Sci. Eng. A*, vol. 111, no. C, pp. 217–225, 1989.

[19] E. M. Fernandes, V. M. Correlo, J. F. Mano, and R. L. Reis, “Novel cork-polymer composites reinforced with short natural coconut fibres: Effect of fibre loading and coupling agent addition,” *Compos. Sci. Technol.*, vol. 78, pp. 56–62, 2013.

[20] T. Forati, M. Atai, A. M. Rashidi, M. Imani, and A. Behnamghader, “Physical and mechanical properties of graphene oxide/polyethersulfone nanocomposites,” *Polym. Adv. Technol.*, vol. 25, no. 3, pp. 322–328, 2014.

[21] S. Qiu, W. Hu, B. Yu, B. Yuan, Y. Zhu, S. Jiang, B. Wang, L. Song, and Y. Hu, “Effect of Functionalized Graphene Oxide with Organophosphorus Oligomer on the Thermal and Mechanical Properties and Fire Safety of Polystyrene,” *Ind. Eng. Chem. Res.*, vol. 54, no. 13, pp. 3309–3319, 2015.

[22] J. Hu and F. Zhang, “Self-assembled fabrication and flame-retardant properties of reduced graphene oxide/waterborne polyurethane nanocomposites,” *J. Therm. Anal. Calorim.*, vol. 118, no. 3, pp. 1561–1568, Aug. 2014.

[23] D. Jariwala, V. K. Sangwan, L. J. Lauhon, T. J. Marks, and M. C. Hersam, “Carbon nanomaterials for electronics, optoelectronics, photovoltaics, and sensing.,” *Chem. Soc. Rev.*, vol. 42, pp. 2824–60, 2013.

[24] D. R. Dreyer, R. S. Ruoff, and C. W. Bielawski, “From conception to realization: An historial account of graphene and some perspectives for its future,” *Angewandte Chemie - International Edition*, vol. 49, no. 49. pp. 9336–9344, 2010.

[25] R. R. Nair, W. Ren, R. Jalil, I. Riaz, V. G. Kravets, L. Britnell, P. Blake, F. Schedin, A. S. Mayorov, S. Yuan, *et al.*, “Fluorographene: A two-dimensional counterpart of Teflon,” *Small*, vol. 6, no. 24, pp. 2877–2884, 2010.

[26] H.-P. Cong, J.-F. Chen, and S.-H. Yu, “Graphene-based macroscopic assemblies and architectures: an emerging material system.,” *Chem. Soc. Rev.*, vol. 43, no. 21, pp. 7295–325, 2014.

[27] V. Singh, D. Joung, L. Zhai, S. Das, S. I. Khondaker, and S. Seal, “Graphene based materials: Past, present and future,” *Prog. Mater. Sci.*, vol. 56, no. 8, pp. 1178–1271, 2011.

[28] A. Reina, X. Jia, J. Ho, D. Nezich, H. Son, V. Bulovic, M. S. Dresselhaus, and K. Jing, "Large area, few-layer graphene films on arbitrary substrates by chemical vapor deposition," *Nano Lett.*, vol. 9, no. 1, pp. 30–35, 2009.

[29] X. Li, W. Cai, J. An, S. Kim, J. Nah, D. Yang, R. Piner, A. Velamakanni, I. Jung, and E. Tutuc, "Large area synthesis of high quality and uniform graphene films on copper foils," *Science (80-.).*, vol. 324, no. 5932, pp. 1312–1314, 2009.

[30] K. S. Subrahmanyam, L. S. Panchakarla, a Govindaraj, and C. N. R. Rao, "Simple Method of Preparing Graphene Flakes by an Arc-Discharge Method Simple Method of Preparing Graphene Flakes by an Arc-Discharge Method," vol. 113, no. February, pp. 4257–4259, 2009.

[31] I. Levchenko, O. Volotskova, A. Shashurin, Y. Raitses, K. Ostrikov, and M. Keidar, "The large-scale production of graphene flakes using magnetically-enhanced arc discharge between carbon electrodes," *Carbon N. Y.*, vol. 48, no. 15, pp. 4570–4574, 2010.

[32] G. M. Rutter, J. N. Crain, N. P. Guisinger, T. Li, P. N. First, and J. a Stroscio, "Scattering and interference in epitaxial graphene.," *Science*, vol. 317, no. 5835, pp. 219–222, 2007.

[33] M. K. Singh, E. Titus, G. Gonçalves, P. a a P. Marques, I. Bdikin, A. L. Kholkin, and J. J. a Gracio, "Atomic-scale observation of rotational misorientation in suspended few-layer graphene sheets.," *Nanoscale*, vol. 2, no. 5, pp. 700–708, 2010.

[34] S. Stankovich, D. A. Dikin, R. D. Piner, K. A. Kohlhaas, A. Kleinhammes, Y. Jia, Y. Wu, S. T. Nguyen, and R. S. Ruoff, "Synthesis of graphene-based nanosheets via chemical reduction of exfoliated graphite oxide," *Carbon N. Y.*, vol. 45, no. 7, pp. 1558–1565, Jun. 2007.

[35] C. Gómez-Navarro, J. C. Meyer, R. S. Sundaram, A. Chuvilin, S. Kurasch, M. Burghard, K. Kern, and U. Kaiser, "Atomic structure of reduced graphene oxide," *Nano Lett.*, vol. 10, no. 4, pp. 1144–1148, 2010.

[36] S. Stankovich, R. D. Piner, X. Chen, N. Wu, S. T. Nguyen, and R. S. Ruoff, "Stable aqueous dispersions of graphitic nanoplatelets via the reduction of exfoliated graphite oxide in the presence of poly(sodium 4-styrenesulfonate)," *J. Mater. Chem.*, vol. 16, no. 2, pp. 155–158, 2006.

[37] G. Goncalves, P. A. A. P. Marques, C. M. Granadeiro, H. I. S. Nogueira, M. K. Singh, and J. Grácio, "Surface modification of graphene nanosheets with gold nanoparticles: The role of oxygen moieties at graphene surface on gold nucleation and growth," *Chem. Mater.*, vol. 21, no. 20, pp. 4796–4802, 2009.

[38] H. C. Schniepp, J. L. Li, M. J. McAllister, H. Sai, M. Herrera-Alonson, D. H. Adamson, R. K. Prud'homme, R. Car, D. A. Seville, and I. A. Aksay, "Functionalized single

graphene sheets derived from splitting graphite oxide," *J. Phys. Chem. B*, vol. 110, no. 17, pp. 8535–8539, 2006.

[39] J. R. Potts, D. R. Dreyer, C. W. Bielawski, and R. S. Ruoff, "Graphene-based polymer nanocomposites," *Polymer (Guildf).*, vol. 52, no. 1, pp. 5–25, 2011.

[40] A. M. Dimiev, J. M. Tour, M. Science, C. Science, N. Science, M. Street, U. States, A. Z. E. Materials, and M. Avenue, "Mechanism of Graphene Oxide," *Am. Chem. Soc.*, vol. 8, no. 3, pp. 3060–3068, 2014.

[41] S. Baksi and S. Biswas, "Nanocomposites – An Overview," *Scitech J.*, vol. 1, no. 5, pp. 22–30, 2014.

[42] D. R. Paul and L. M. Robeson, "Polymer nanotechnology: Nanocomposites," *Polymer (Guildf).*, vol. 49, no. 15, pp. 3187–3204, Jul. 2008.

[43] D. Konios, M. M. Stylianakis, E. Stratakis, and E. Kymakis, "Dispersion behaviour of graphene oxide and reduced graphene oxide.," *J. Colloid Interface Sci.*, vol. 430, pp. 108–12, Sep. 2014.

[44] Y. Zhu, S. Murali, W. Cai, X. Li, J. W. Suk, J. R. Potts, and R. S. Ruoff, "Graphene and graphene oxide: Synthesis, properties, and applications," *Adv. Mater.*, vol. 22, no. 35, pp. 3906–3924, 2010.

[45] C. Galande, W. Gao, A. Mathkar, A. M. Dattelbaum, T. N. Narayanan, A. D. Mohite, and P. M. Ajayan, "Science and Engineering of Graphene Oxide," *Part. Part. Syst. Charact.*, vol. 31, no. 6, pp. 619–638, 2014.

[46] J. Alongi, F. Carosio, and G. Malucelli, "Current emerging techniques to impart flame retardancy to fabrics: An overview," *Polym. Degrad. Stab.*, vol. 106, pp. 138–149, Aug. 2014.

[47] J. Jordan, K. I. Jacob, R. Tannenbaum, M. A. Sharaf, and I. Jasiuk, "Experimental trends in polymer nanocomposites - A review," *Mater. Sci. Eng. A*, vol. 393, no. 1–2, pp. 1–11, 2005.

[48] S. I. Abdullah and M. N. M. Ansari, "Mechanical properties of graphene oxide (GO)/epoxy composites," *HBRC J.*, vol. 11, no. 2, pp. 151–156, Aug. 2015.

[49] D. R. Bortz, E. G. Heras, and I. Martin-Gullon, "Impressive Fatigue Life and Fracture Toughness Improvements in Graphene Oxide/Epoxy Composites," *Macromolecules*, vol. 45, no. 1, pp. 238–245, Jan. 2012.

[50] Y. J. Wan, L. C. Tang, L. X. Gong, D. Yan, Y. B. Li, L. Bin Wu, J. X. Jiang, and G. Q. Lai, "Grafting of epoxy chains onto graphene oxide for epoxy composites with improved mechanical and thermal properties," *Carbon N. Y.*, vol. 69, pp. 467–480, Apr. 2014.

[51] B. Zhang, R. Asmatulu, S. a. Soltani, L. N. Le, and S. S. a. Kumar, "Mechanical and thermal properties of hierarchical composites enhanced by pristine graphene and graphene

oxide nanoinclusions," *J. Appl. Polym. Sci.*, vol. 131, no. 19, p. n/a-n/a, Oct. 2014.

[52] R. Wang, D. Zhuo, Z. Weng, L. Wu, X. Cheng, Y. Zhou, J. Wang, and B. Xuan, "A novel nanosilica/graphene oxide hybrid and its flame retarding epoxy resin with simultaneously improved mechanical, thermal conductivity, and dielectric properties," *J. Mater. Chem. A*, vol. 3, no. 18, pp. 9826–9836, 2015.

[53] K. Balasubramanian, "Reinforcement of poly ether sulphones (PES) with exfoliated graphene oxide for aerospace applications," *IOP Conf. Ser. Mater. Sci. Eng.*, vol. 40, p. 12022, 2012.

[54] J. Zhang, C. Zhang, and S. A. Madbouly, "In situ polymerization of bio-based thermosetting polyurethane/graphene oxide nanocomposites," *J. Appl. Polym. Sci.*, vol. 132, no. 13, p. n/a-n/a, 2015.

[55] T. Kuilla, S. Bhadra, D. Yao, N. H. Kim, S. Bose, and J. H. Lee, "Recent advances in graphene based polymer composites," *Prog. Polym. Sci.*, vol. 35, no. 11, pp. 1350–1375, Nov. 2010.

[56] J. Wang, Z. Li, G. Fan, H. Pan, Z. Chen, and D. Zhang, "Reinforcement with graphene nanosheets in aluminum matrix composites," *Scr. Mater.*, vol. 66, no. 8, pp. 594–597, 2012.

[57] S. A. Song, Y. S. Chung, and S. S. Kim, "The mechanical and thermal characteristics of phenolic foams reinforced with carbon nanoparticles," *Compos. Sci. Technol.*, vol. 103, pp. 85–93, 2014.

[58] B. Wicklein, A. Kocjan, G. Salazar-Alvarez, F. Carosio, G. Camino, M. Antonietti, and L. Bergström, "Thermally insulating and fire-retardant lightweight anisotropic foams based on nanocellulose and graphene oxide," *Nat. Nanotechnol.*, pp. 1–7, 2014.

[59] J. Zhou, Z. Yao, Y. Chen, D. Wei, and T. Xu, "Fabrication and mechanical properties of phenolic foam reinforced with graphene oxide," *Polym. Compos.*, vol. 35, no. 3, pp. 581–586, 2014.

[60] G. Yang, J. Su, J. Gao, X. Hu, C. Geng, and Q. Fu, "Fabrication of well-controlled porous foams of graphene oxide modified poly(propylene-carbonate) using supercritical carbon dioxide and its potential tissue engineering applications," *J. Supercrit. Fluids*, vol. 73, pp. 1–9, 2013.

[61] M. Li, P. Cheng, R. Zhang, G. Luo, Q. Shen, and L. Zhang, "Preparation of PMMA/graphene oxide microcellular foams using supercritical carbon dioxide," *IOP Conf. Ser. Mater. Sci. Eng.*, vol. 87, p. 12042, 2015.

[62] E. Zegeye, A. K. Ghamsari, and E. Woldesenbet, "Composites : Part B Mechanical properties of graphene platelets reinforced syntactic foams," *Compos. PART B*, vol. 60, pp. 268–273, 2014.

[63] X. Zhao, Q. Zhang, D. Chen, and P. Lu, “Enhanced Mechanical Properties of Graphene-Based Poly (vinyl alcohol) Composites,” pp. 2357–2363, 2010.

[64] J. Liang, Y. Xu, Y. Huang, L. Zhang, Y. Wang, Y. Ma, F. Li, T. Guo, and Y. Chen, “Infrared-Triggered Actuators from Graphene-Based Nanocomposites,” pp. 9921–9927, 2009.

[65] M. Antunes and J. I. Velasco, “Multifunctional polymer foams with carbon nanoparticles,” *Progress in Polymer Science*, vol. 39, no. 3. pp. 486–509, 2014.

[66] C. A. W. Alexander B. Morgan, *Flame Retardant Polymer Nanocomposites*, John Wiley. Hoboken, NJ, USA: John Wiley & Sons, Inc., 2007.

[67] P. Kiliaris and C. D. Papaspyrides, “Polymer/layered silicate (clay) nanocomposites: An overview of flame retardancy,” *Prog. Polym. Sci.*, vol. 35, no. 7, pp. 902–958, 2010.

[68] P. Zhang, Y. Hu, L. Song, J. Ni, W. Xing, and J. Wang, “Effect of expanded graphite on properties of high-density polyethylene/paraffin composite with intumescent flame retardant as a shape-stabilized phase change material,” *Sol. Energy Mater. Sol. Cells*, vol. 94, no. 2, pp. 360–365, 2010.

[69] Q. Zhang, J. Zhan, K. Zhou, H. Lu, W. Zeng, A. a. Stec, T. R. Hull, Y. Hu, and Z. Gui, “The influence of carbon nanotubes on the combustion toxicity of PP/intumescent flame retardant composites,” *Polym. Degrad. Stab.*, vol. 115, pp. 38–44, 2015.

[70] G. Beyer, “Carbon Nanotubes as a New Class of Flame Retardants for Polymers,” *Wire Cable Technol. Int.*, vol. 32, no. 6, pp. 60–63, 2004.

[71] G. Beyer, “Short Communication : Carbon Nanotubes as Flame Retardants for Polymers,” *Fire Mater.*, vol. 26, pp. 291–293, 2002.

[72] T. Kashiwagi, F. Du, J. F. Douglas, K. I. Winey, R. H. Harris, and J. R. Shields, “Nanoparticle networks reduce the flammability of polymer nanocomposites.,” *Nat. Mater.*, vol. 4, no. 12, pp. 928–33, 2005.

[73] T. Kashiwagi, F. Du, K. I. Winey, K. M. Groth, J. R. Shields, S. P. Bellayer, H. Kim, and J. F. Douglas, “Flammability properties of polymer nanocomposites with single-walled carbon nanotubes: effects of nanotube dispersion and concentration,” *Polymer (Guildf).*, vol. 46, no. 2, pp. 471–481, 2005.

[74] T. Kashiwagi, E. Grulke, J. Hilding, K. Groth, R. Harris, K. Butler, J. Shields, S. Kharchenko, and J. Douglas, “Thermal and flammability properties of polypropylene/carbon nanotube nanocomposites,” *Polymer (Guildf).*, vol. 45, no. 12, pp. 4227–4239, 2004.

[75] B. Yu, Y. Shi, B. Yuan, S. Qiu, W. Xing, W. Hu, L. Song, S. Lo, and Y. Hu, “Enhanced thermal and flame retardant properties of flame-retardant-wrapped graphene/epoxy resin

nanocomposites," *J. Mater. Chem. A*, vol. 3, no. 15, pp. 8034–8044, 2015.

[76] G. Huang, J. Gao, X. Wang, H. Liang, and C. Ge, "How can graphene reduce the flammability of polymer nanocomposites?," *Mater. Lett.*, vol. 66, no. 1, pp. 187–189, 2012.

[77] B. Sang, Z. Li, X. Li, L. Yu, and Z. Zhang, "Graphene-based flame retardants : a review," *J. Mater. Sci.*, vol. 51, no. 18, pp. 8271–8295, 2016.

[78] A. L. Higginbotham, J. R. Lomeda, A. B. Morgan, and J. M. Tour, "Graphite oxide flame-retardant polymer nanocomposites," *ACS Appl. Mater. Interfaces*, vol. 1, no. 10, pp. 2256–2261, 2009.

[79] Z. Wang, X. Z. Tang, Z. Z. Yu, P. Guo, H. H. Song, and X. S. Duc, "Dispersion of graphene oxide and its flame retardancy effect on epoxy nanocomposites," *Chinese J. Polym. Sci. (English Ed.*, vol. 29, no. 3, pp. 368–376, 2011.

[80] J. Wang and Z. Han, "The combustion behavior of polyacrylate ester/graphite oxide composites," *Polym. Adv. Technol.*, vol. 17, no. 4, pp. 335–340, 2006.

[81] J. Xu, J. Liu, and K. Li, "Application of Functionalized Graphene Oxide in Flame-Retardant Polypropylene," *J. Vinyl Addit. Technol.*, 2014.

[82] R. Harris, T. J. Ohlemiller, M. Zammarano, R. H. Kra, J. R. Shields, S. S. Rahatekar, S. Lacerda, and J. W. Gilman, "Flammability reduction of flexible polyurethane foams via carbon nanofiber network formation," no. May, pp. 588–595, 2008.

[83] D. K. Chattopadhyay and D. C. Webster, "Thermal stability and flame retardancy of polyurethanes," *Progress in Polymer Science (Oxford)*, vol. 34, no. 10. pp. 1068–1133, 2009.

[84] L. Chen, D. Rende, L. S. Schadler, and R. Ozisik, "Polymer nanocomposite foams," *J. Mater. Chem. A*, vol. 1, no. 12, pp. 3837–3848, 2013.

[85] F. Laoutid, L. Bonnaud, M. Alexandre, J. M. Lopez-Cuesta, and P. Dubois, "New prospects in flame retardant polymer materials: From fundamentals to nanocomposites," *Materials Science and Engineering R: Reports*, vol. 63, no. 3. pp. 100–125, 2009.

[86] C. Bao, L. Song, W. Xing, B. Yuan, C. a. Wilkie, J. Huang, Y. Guo, and Y. Hu, "Preparation of graphene by pressurized oxidation and multiplex reduction and its polymer nanocomposites by masterbatch-based melt blending," *J. Mater. Chem.*, vol. 22, no. 13, p. 6088, 2012.

[87] T. R. Hull, J. Wang, and Y. Hu, "E ff ect of Functionalized Graphene Oxide with Hyper-Branched Flame Retardant on Flammability and Thermal Stability of Cross-Linked Polyethylene," 2014.

[88] W. Hu, B. Yu, S. D. Jiang, L. Song, Y. Hu, and B. Wang, "Hyper-branched polymer grafting graphene oxide as an effective flame retardant and smoke suppressant for

polystyrene," *J. Hazard. Mater.*, vol. 300, pp. 58–66, 2015.

[89] B. Yuan, H. Sheng, X. Mu, L. Song, Q. Tai, Y. Shi, K. M. Liew, and Y. Hu, "Enhanced flame retardancy of polypropylene by melamine-modified graphene oxide," *J. Mater. Sci.*, vol. 50, no. 16, pp. 5389–5401, 2015.

[90] G. Huang, S. Chen, S. Tang, and J. Gao, "A novel intumescent flame retardant-functionalized graphene: Nanocomposite synthesis, characterization, and flammability properties," *Mater. Chem. Phys.*, vol. 135, no. 2–3, pp. 938–947, 2012.

[91] M. Saenz-Perez, E. Lizundia, J. M. Laza, J. Garcia-Barrasa, J. L. Vilas, and L. M. Leon, "Methylene diphenyl diisocyanate (MDI) and toluene diisocyanate (TDI) based polyurethanes: thermal, shape-memory and mechanical behavior," *RSC Adv.*, vol. 6, no. 73, pp. 69094–69102, 2016.

Annex A

Stress-strain curves from second dynamic impact

Influence of the agglomerating agent

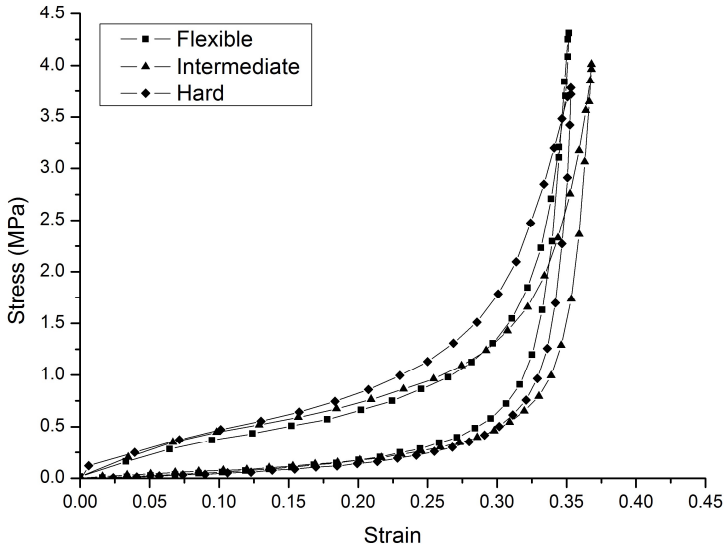

Figure A.1: Influence of the agglomerating agent on the second impact (same type of grain, density (200kg/m^3) and 15 wt.% binding agent).

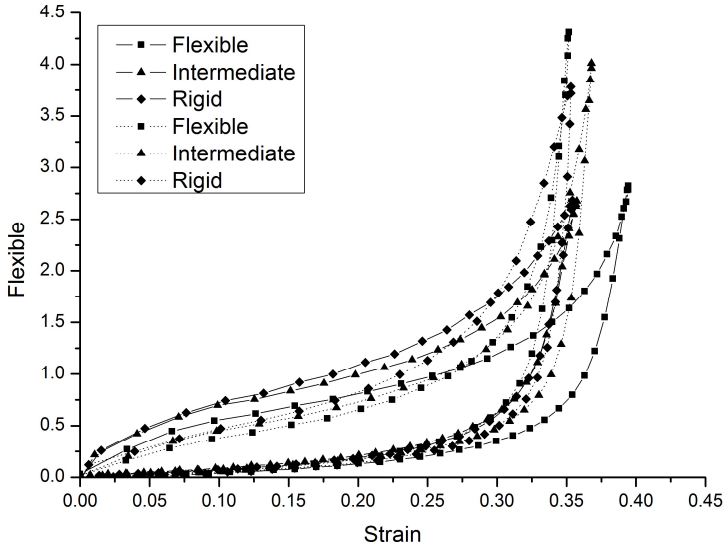

Figure A.2: Influence of the agglomerating agent from the first to the second impact (same type of grain, density (200kg/m^3) and 15 wt.% binding agent).

Influence of the percentage of agglomerating agent

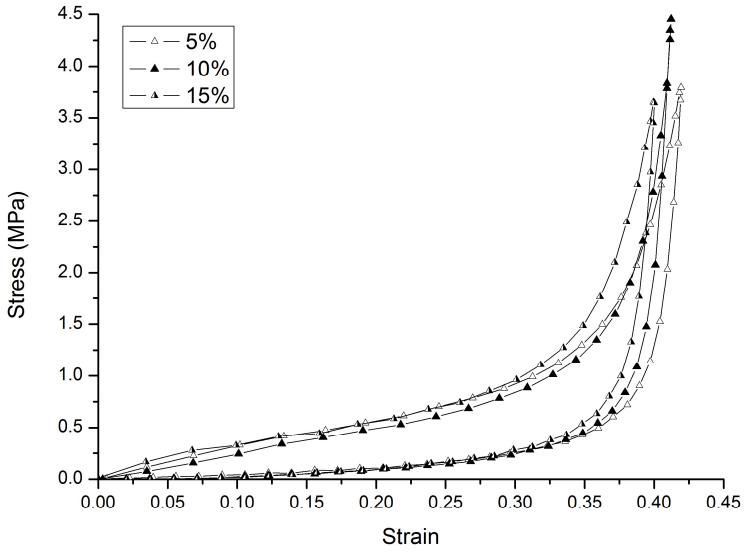

Figure A.3: Influence of the agglomerating agent on the second impact (same type of grain, density (200kg/m^3) and 15 wt.% binding agent).

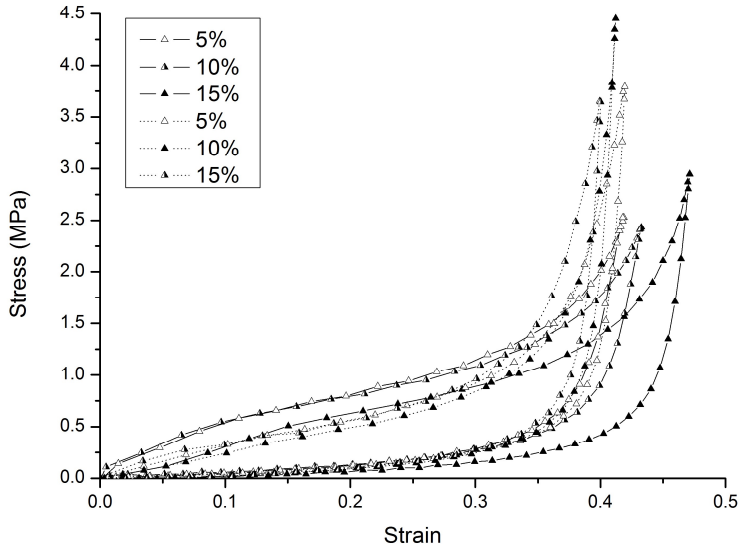

Figure A.4: Influence of the agglomerating agent from the first to the second impact (same type of grain, density (200kg/m^3) and 15 wt.% binding agent).

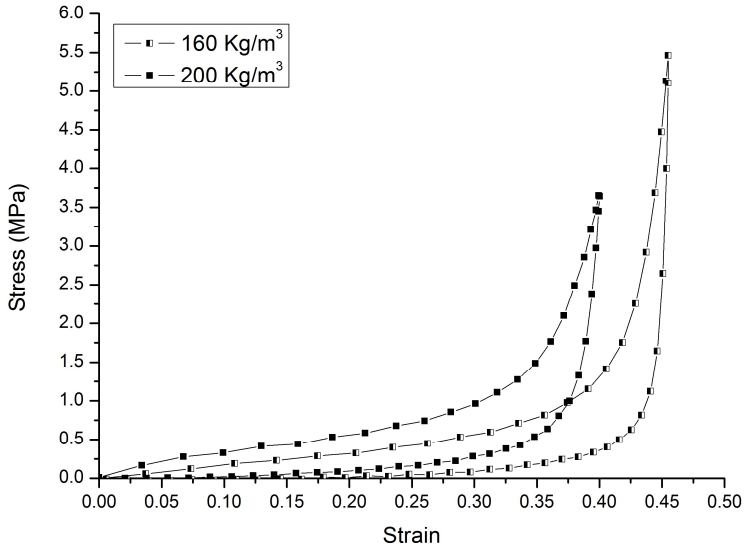

Figure A.5: Influence of the agglomerating agent on the second impact (same type of grain, density (200kg/m^3) and 15 wt.% binding agent).

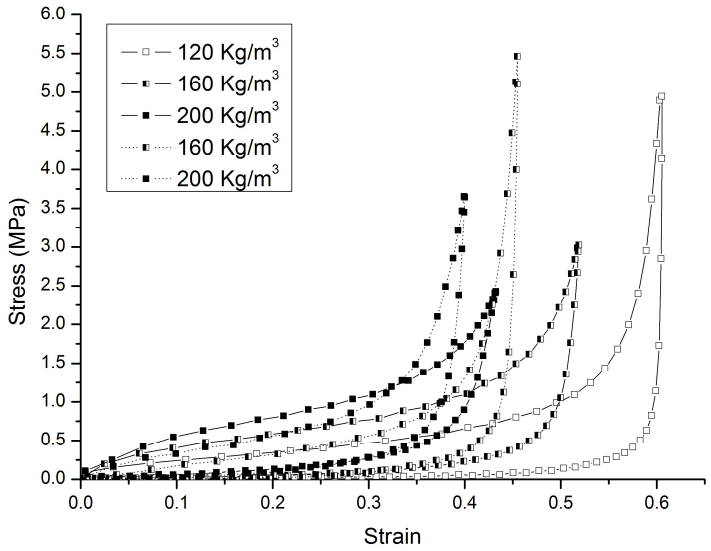

Figure A.6: Influence of the agglomerating agent from the first to the second impact (same type of grain, density (200kg/m^3) and 15 wt.% binding agent).

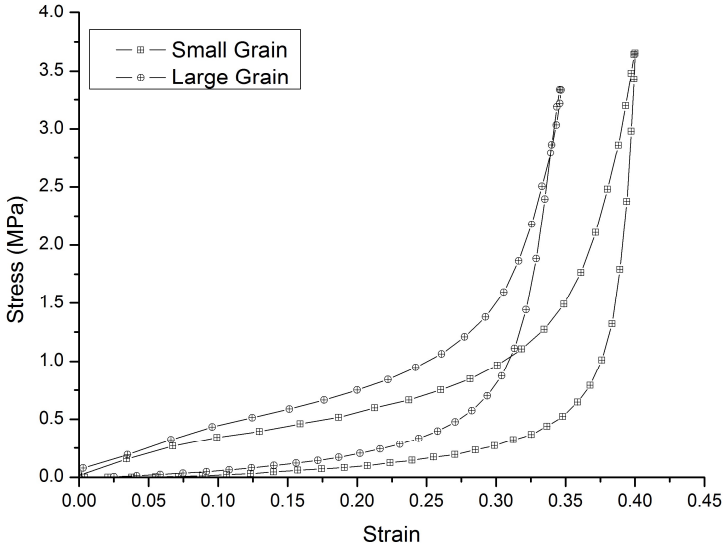

Figure A.7: Influence of the agglomerating agent on the second impact (same type of grain, density (200kg/m^3) and 15 wt.% binding agent).

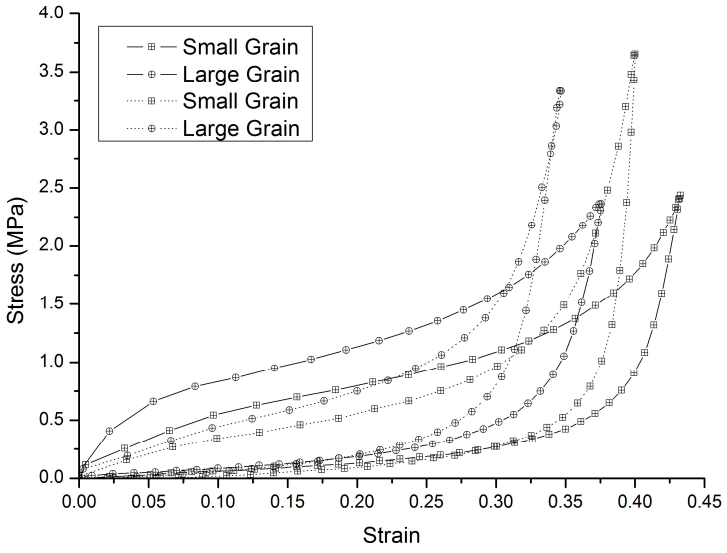

Figure A.8: Influence of the agglomerating agent from the first to the second impact (same type of grain, density (200kg/m^3) and 15 wt.% binding agent).

Values of acceleration and displacement

Influence of the agglomerating agent

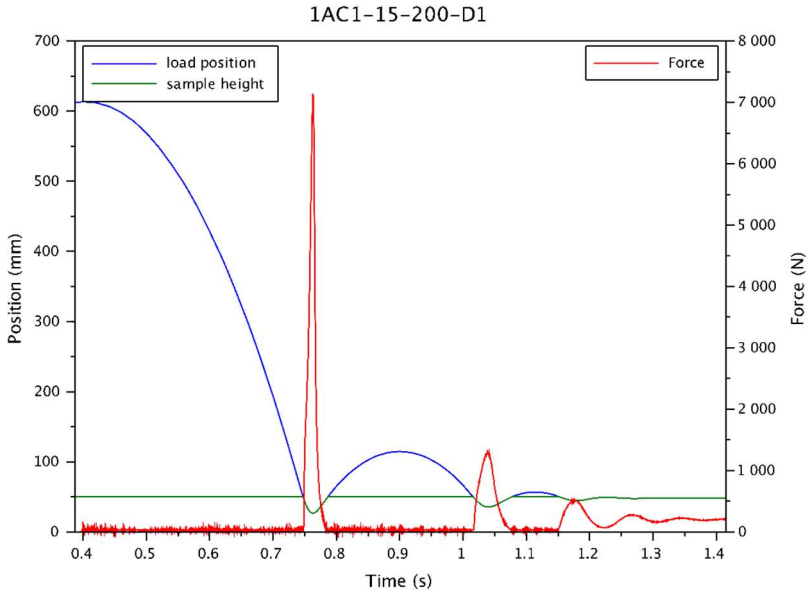

Figure A.9: First impact for the sample with small grain (0.5-1mm), density (200kg/m^3) and 15 wt.% of flexible binder.

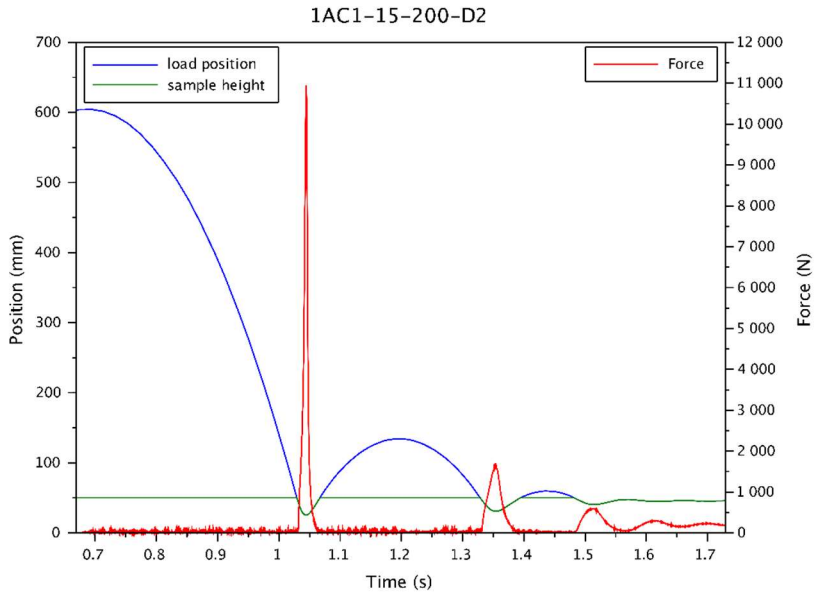

Figure A.10: Second impact for the sample with small grain (0.5-1mm), density (200kg/m^3) and 15 wt.% of flexible binder.

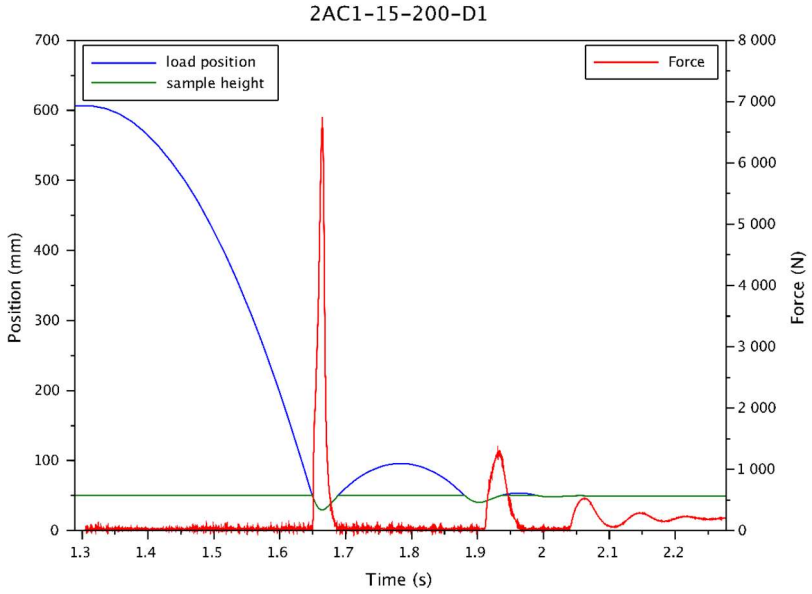

Figure A.11: First impact for the sample with small grain (0.5-1mm), density (200kg/m^3) and 15 wt.% of intermediate binder.

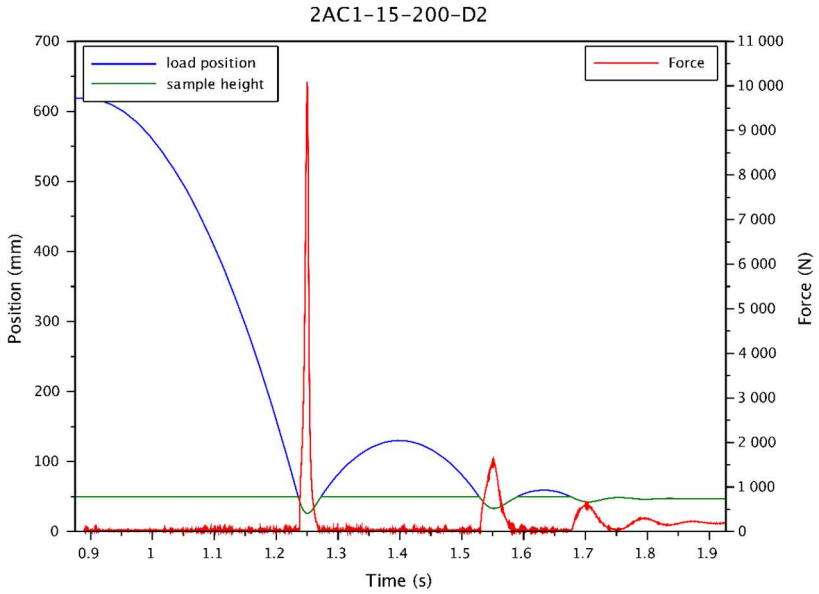

Figure A.12: Second impact for the sample with small grain (0.5-1mm), density (200kg/m^3) and 15 wt.% of intermediate binder.

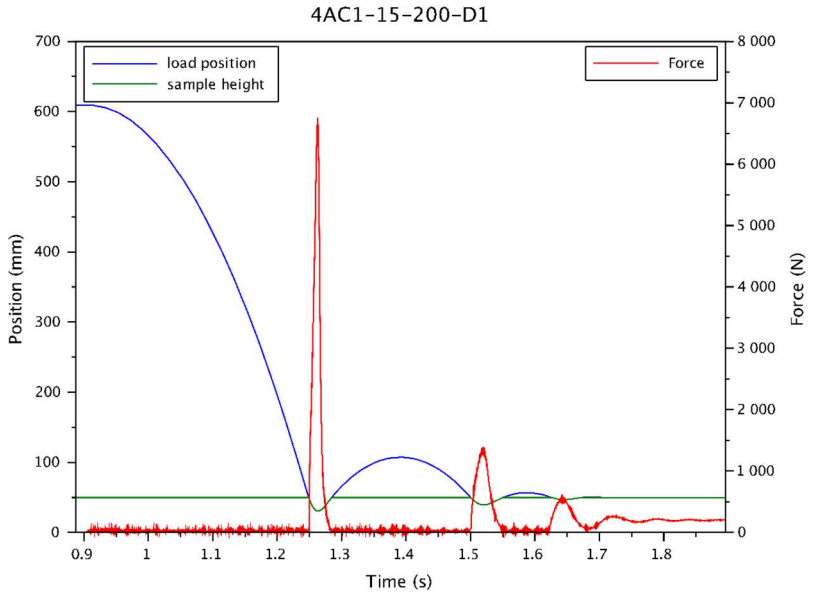

Figure A.13: First impact for the sample with small grain (0.5-1mm), density (200kg/m^3) and 15 wt.% of hard binder.

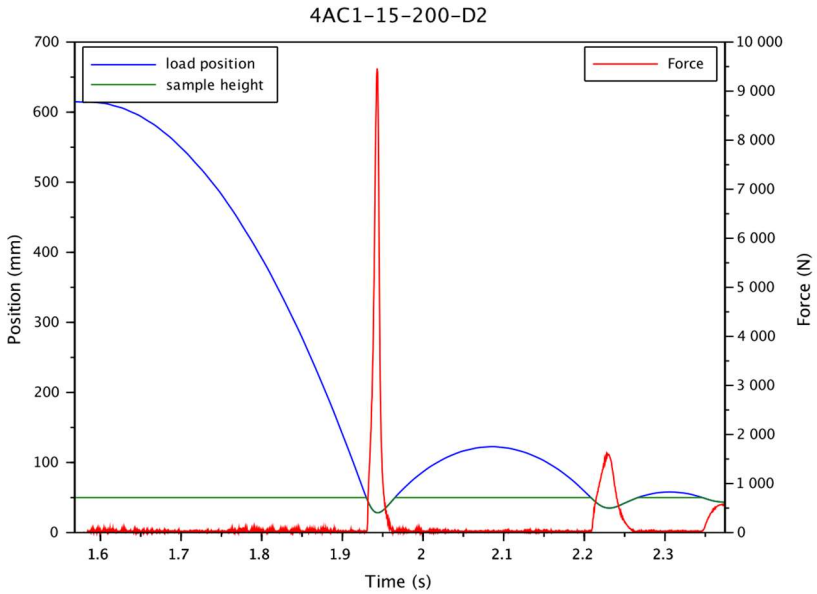

Figure A.14: Second impact for the sample with small grain (0.5-1mm), density (200kg/m^3) and 15 wt.% of hard binder.

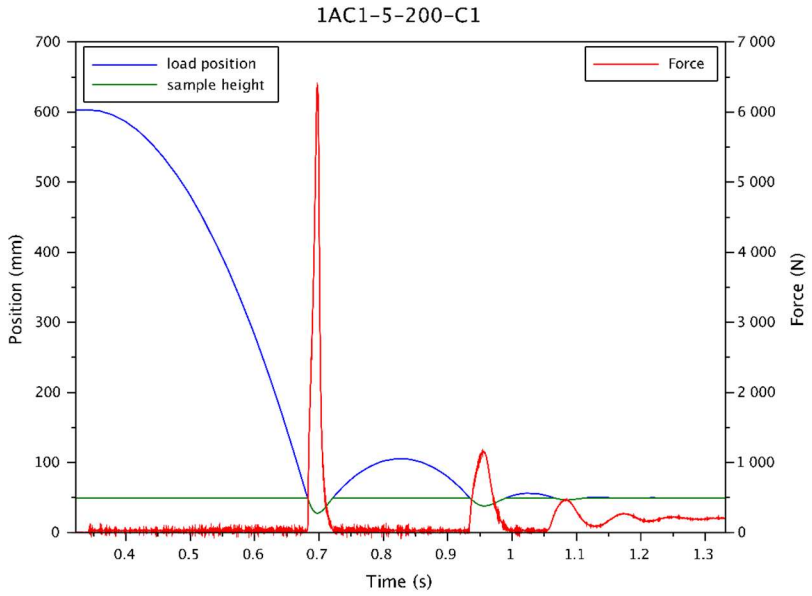

Figure A.15: First impact for the sample with small grain (0.5-1mm), density (200kg/m^3) and 5 wt.% of flexible binder.

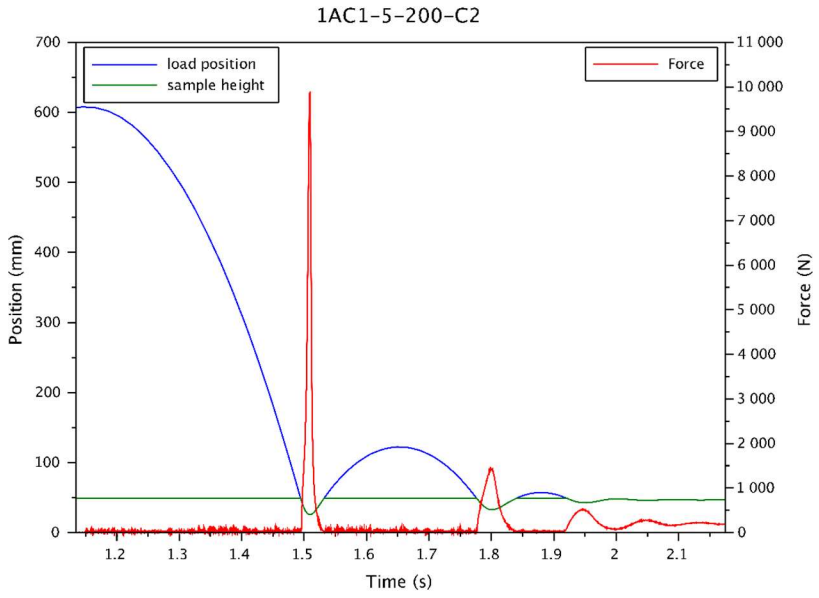

Figure A.16: Second impact for the sample with small grain (0.5-1mm), density (200kg/m^3) and 5 wt.% of flexible binder.

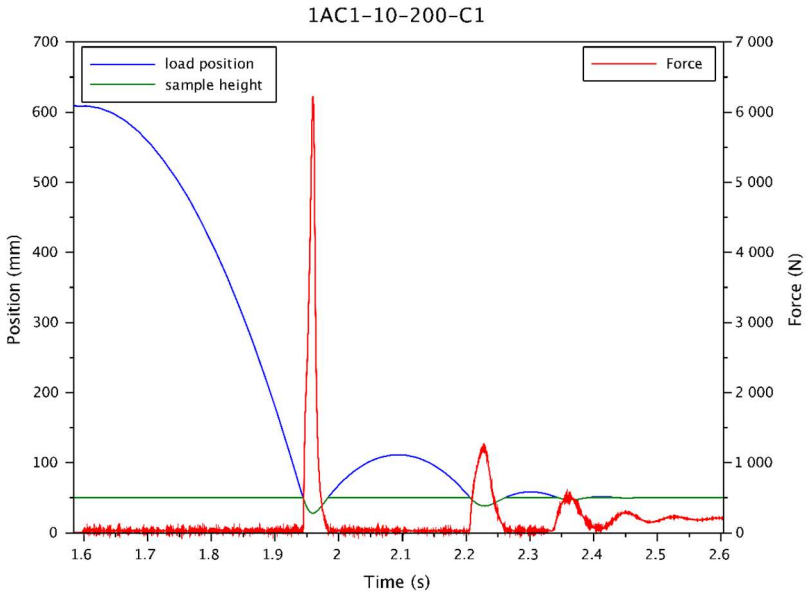

Figure A.17: First impact for the sample with small grain (0.5-1mm), density (200kg/m^3) and 10 wt.% of flexible binder.

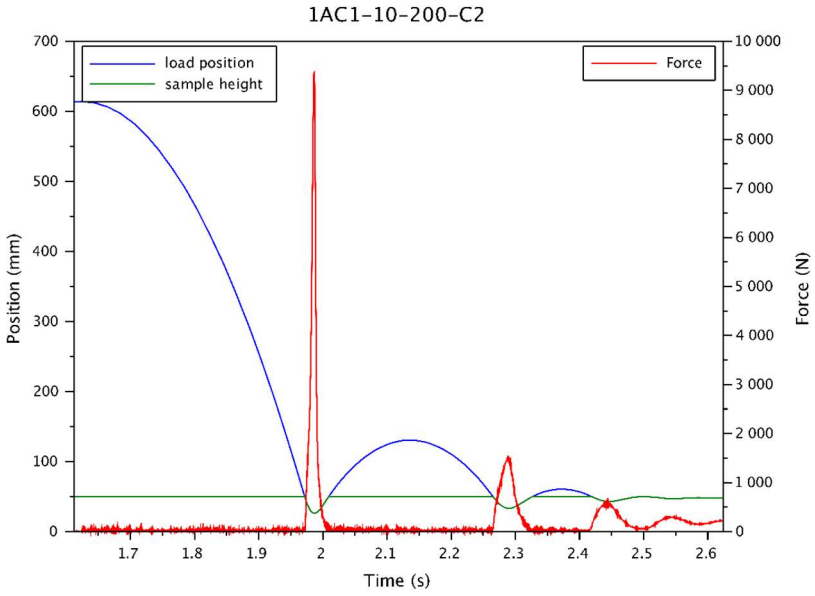

Figure A.18: Second impact for the sample with small grain (0.5-1mm), density (200kg/m^3) and 10 wt.% of flexible binder.

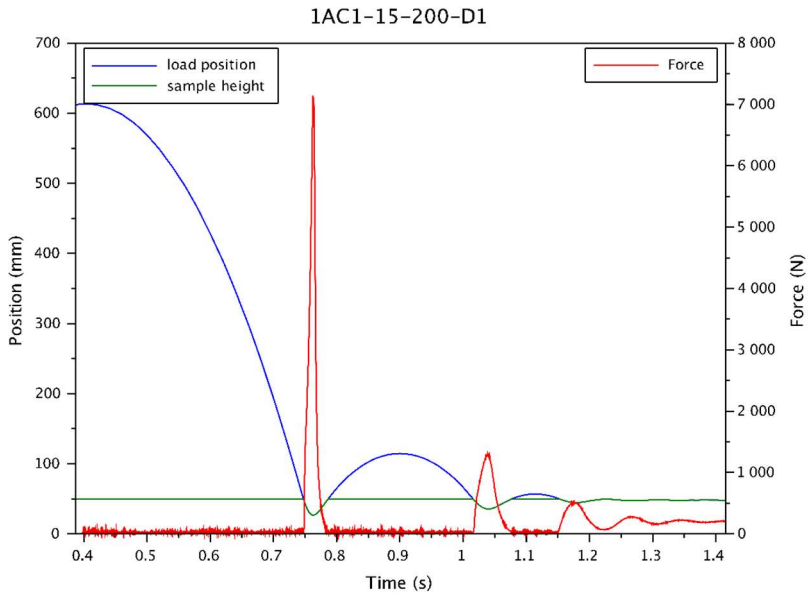

Figure A.19: First impact for the sample with small grain (0.5-1mm), density (200kg/m^3) and 15 wt.% of flexible binder.

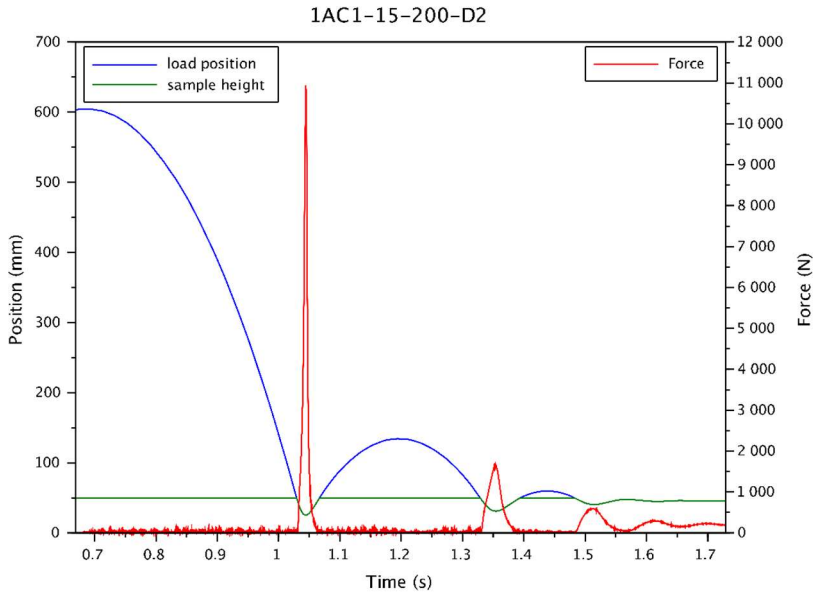

Figure A.20: Second impact for the sample with small grain (0.5-1mm), density (200kg/m^3) and 15 wt.% of flexible binder.

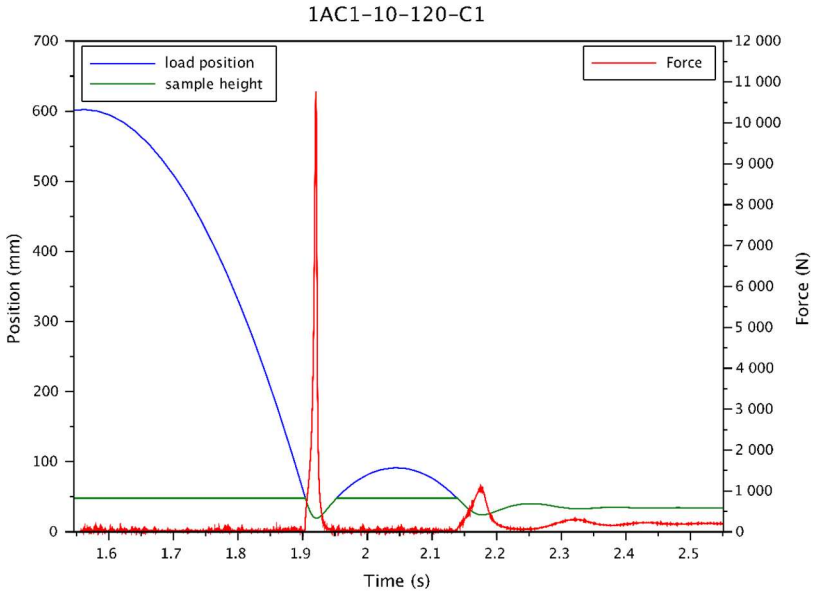

Figure A.21: First impact for the sample with small grain (0.5-1mm), density (120kg/m^3) and 10 wt.% of flexible binder.

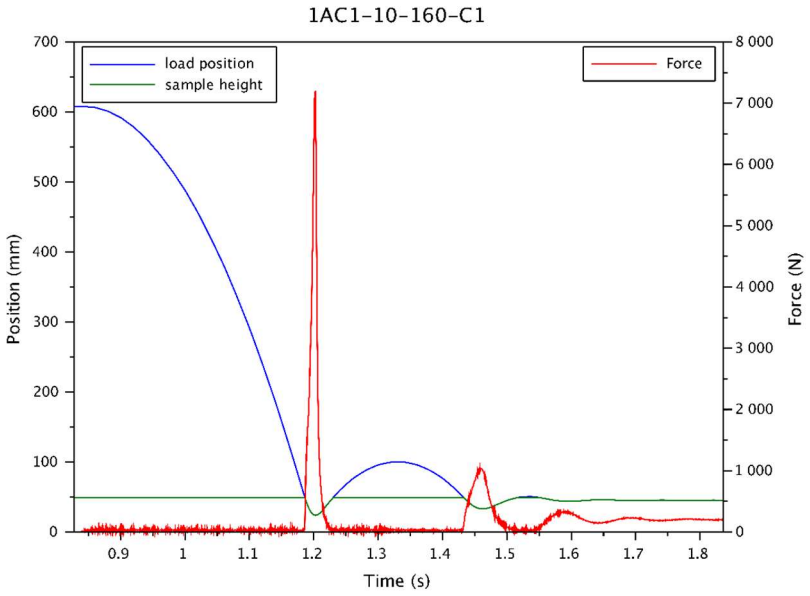

Figure A.22: First impact for the sample with small grain (0.5-1mm), density (160kg/m^3) and 10 wt.% of flexible binder.

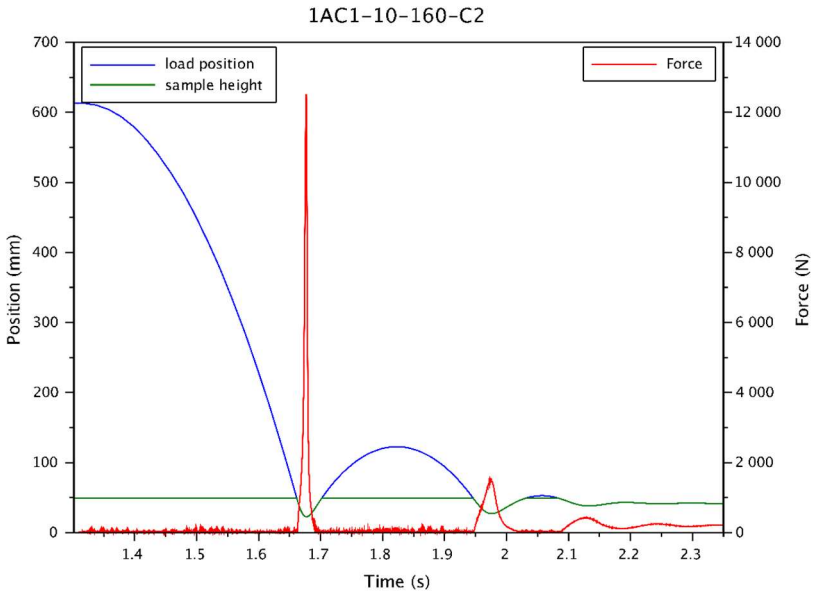

Figure A.23: Second impact for the sample with small grain (0.5-1mm), density (160kg/m^3) and 10 wt.% of flexible binder.

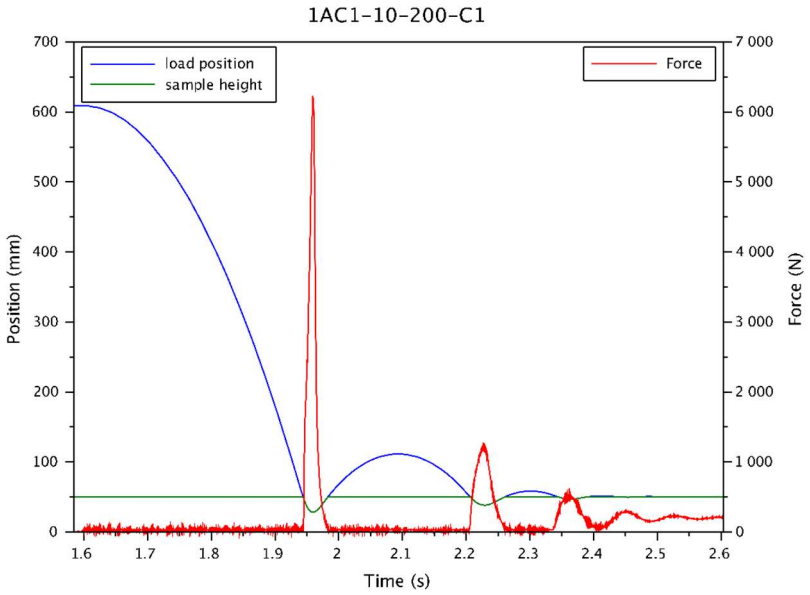

Figure A.24: First impact for the sample with small grain (0.5-1mm), density (200kg/m^3) and 10 wt.% of flexible binder.

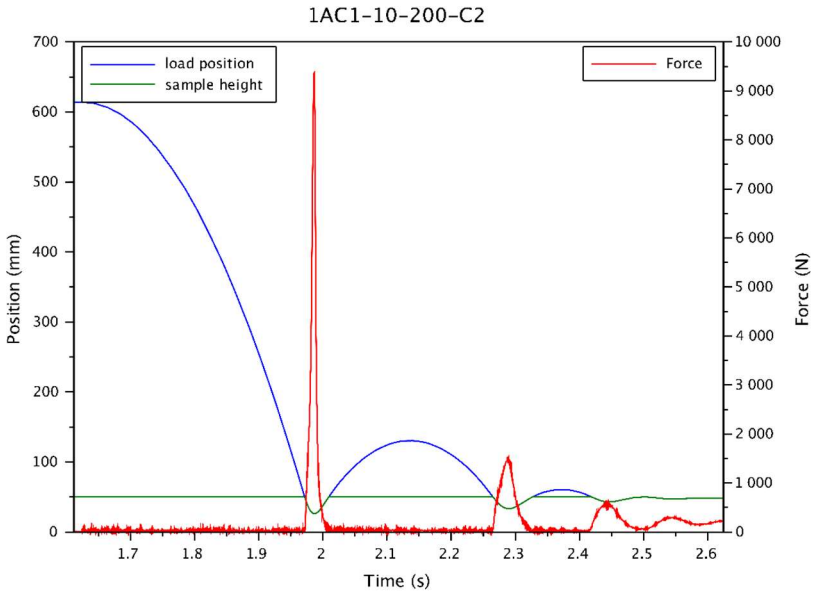

Figure A.25: Second impact for the sample with small grain (0.5-1mm), density (200kg/m^3) and 10 wt.% of flexible binder.

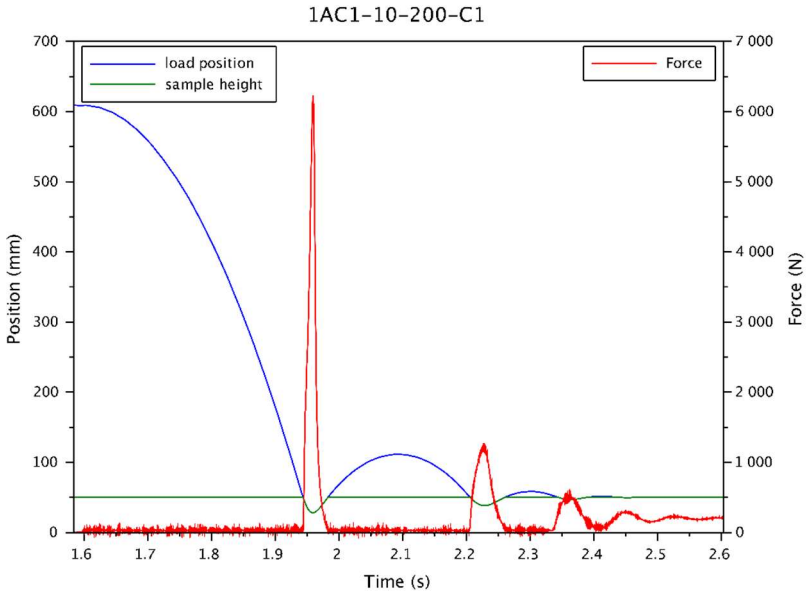

Figure A.26: First impact for the sample with small grain (0.5-1mm), density (200kg/m^3) and 10 wt.% of flexible binder.

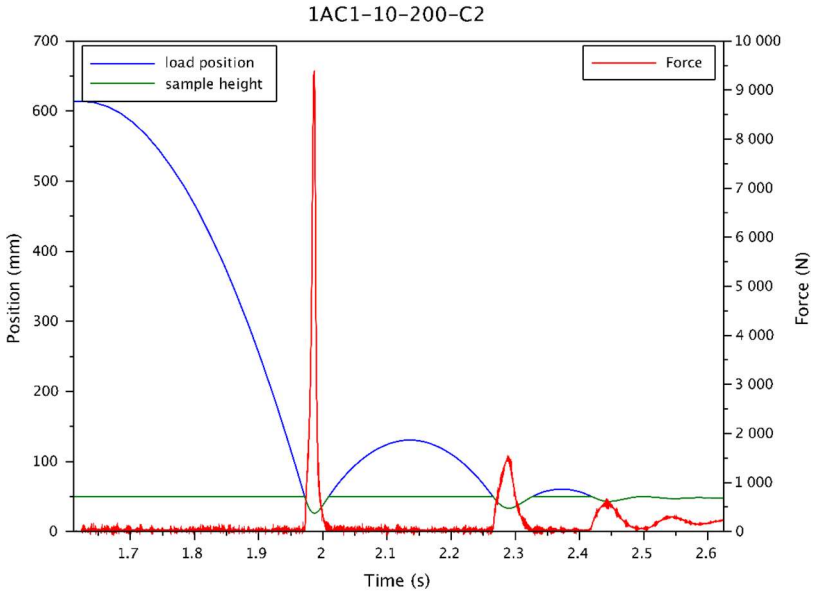

Figure A.27: Second impact for the sample with small grain (0.5-1mm), density (200kg/m^3) and 10 wt.% of flexible binder.

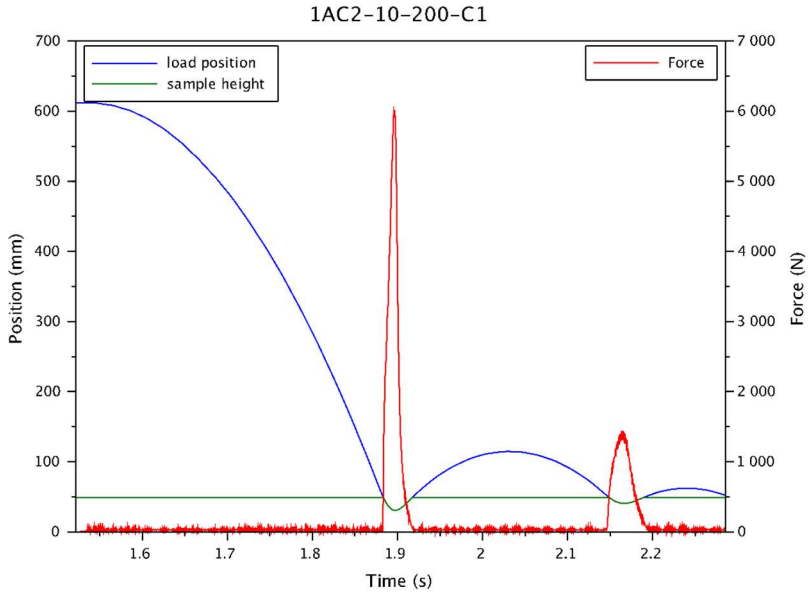

Figure A.28: First impact for the sample with large grain (3-4mm), density (200kg/m^3) and 10 wt.% of flexible binder.

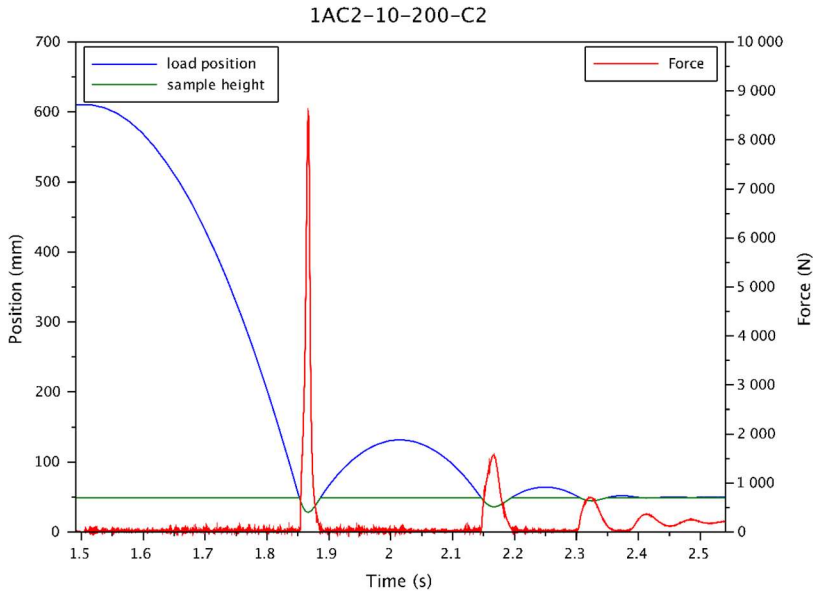

Figure A.29: Second impact for the sample with large grain (3-4mm), density (200kg/m^3) and 10 wt.% of flexible binder.